

Finite-Width Effects in Three-Body B Decays

Hai-Yang Cheng¹, Cheng-Wei Chiang², Chun-Khiang Chua³

¹ Institute of Physics, Academia Sinica
Taipei, Taiwan 115, Republic of China

² Department of Physics, National Taiwan University
Taipei, Taiwan 106, Republic of China

³ Department of Physics and Center for High Energy Physics
Chung Yuan Christian University
Chung-Li, Taiwan 320, Republic of China

Abstract

It is customary to apply the so-called narrow width approximation $\Gamma(B \rightarrow RP_3 \rightarrow P_1P_2P_3) = \Gamma(B \rightarrow RP_3)\mathcal{B}(R \rightarrow P_1P_2)$ to extract the branching fraction of the quasi-two-body decay $B \rightarrow RP_3$, with R and P_3 being an intermediate resonant state and a pseudoscalar meson, respectively. However, the above factorization is valid only in the zero width limit. We consider a correction parameter η_R from finite width effects. Our main results are: (i) We present a general framework for computing η_R and show that it can be expressed in terms of the normalized differential rate and determined by its value at the resonance. (ii) We introduce a form factor $F(s_{12}, m_R)$ for the strong coupling involved in the $R(m_{12}) \rightarrow P_1P_2$ decay when m_{12} is away from m_R . We find that off-shell effects are small in vector meson productions, but prominent in the $K_2^*(1430)$, $\sigma/f_0(500)$ and $K_0^*(1430)$ resonances. (iii) We evaluate η_R in the theoretical framework of QCD factorization (QCDF) and in the experimental parameterization (EXPP) for three-body decay amplitudes. In general, η_R^{QCDF} and η_R^{EXPP} are similar for vector mesons, but different for tensor and scalar resonances. A study of the differential rates enables us to understand the origin of their differences. (iv) Finite-width corrections to $\mathcal{B}(B^- \rightarrow RP)_{\text{NWA}}$ obtained in the narrow width approximation are generally small, less than 10%, but they are prominent in $B^- \rightarrow \sigma/f_0(500)\pi^-$ and $B^- \rightarrow \bar{K}_0^{*0}(1430)\pi^-$ decays. The EXPP of the normalized differential rates should be contrasted with the theoretical predictions from QCDF calculation as the latter properly takes into account the energy dependence in weak decay amplitudes. (v) It is common to use the Gounaris-Sakurai model to describe the line shape of the broad $\rho(770)$ resonance. After including finite-width effects, the PDG value of $\mathcal{B}(B^- \rightarrow \rho\pi^-) = (8.3 \pm 1.2) \times 10^{-6}$ should be corrected to $(7.9 \pm 1.1) \times 10^{-6}$ in EXPP and $(7.7 \pm 1.1) \times 10^{-6}$ in QCDF. (vi) For the very broad $\sigma/f_0(500)$ scalar resonance, we use a simple pole model to describe its line shape and find a very large width effect: $\eta_\sigma^{\text{QCDF}} \sim 2.15$ and $\eta_\sigma^{\text{EXPP}} \sim 1.64$. Consequently, $B^- \rightarrow \sigma\pi^-$ has a large branching fraction of order 10^{-5} . (vii) We employ the Breit-Wigner line shape to describe the production of $K_0^*(1430)$ in three-body B decays and find large off-shell effects. The smallness of $\eta_{K_0^*}^{\text{QCDF}}$ relative to $\eta_{K_0^*}^{\text{EXPP}}$ is ascribed to the differences in the normalized differential rates off the resonance. (viii) In the approach of QCDF, the calculated CP asymmetries of $B^- \rightarrow f_2(1270)\pi^-$, $\sigma/f_0(500)\pi^-$, $K^-\rho^0$ decays agree with the experimental observations. The non-observation of CP asymmetry in $B^- \rightarrow \rho(770)\pi^-$ can also be accommodated in QCDF.

Contents

I. Introduction	3
II. General Framework	5
A. Scalar intermediate states	5
B. General case	6
C. η_R and the normalized differential rate	8
D. Formula of η_R in the case of the Gounaris-Sakurai line shape	9
E. Formula of η_R in the case of the $\sigma/f_0(500)$ resonance	10
III. Differential rates and η_R^{EXP} using the experimental parameterization	11
IV. Analysis in the QCD factorization approach	13
A. Tensor resonances	14
1. $f_2(1270)$	14
2. $K_2^*(1430)$	21
B. Vector mesons	23
1. $\rho(770)\pi^-$	23
2. $\rho(770)K^-$	27
3. $K^*(892)$	28
C. Scalar resonances	30
1. $\sigma/f_0(500)$	30
2. $K_0^*(1430)$	33
V. Discussions	36
A. Finite-width and off-shell effects	36
B. Branching fractions of quasi-two-body decays	39
VI. Conclusions	40
Acknowledgments	42
References	42

I. INTRODUCTION

In a three-body decay with resonance contributions, it is a common practice to apply the factorization relation, also known as the narrow width approximation (NWA), to factorize the process as a quasi-two-body weak decay followed by another two-body strong decay. Take a B meson decay $B \rightarrow RP_3 \rightarrow P_1P_2P_3$ as an example, where R and P_3 are an intermediate resonant state and a pseudoscalar meson, respectively. One then uses

$$\Gamma(B \rightarrow RP_3 \rightarrow P_1P_2P_3) = \Gamma(B \rightarrow RP_3)\mathcal{B}(R \rightarrow P_1P_2), \quad (1.1)$$

to extract the branching fraction of the quasi-two-body decay, $\mathcal{B}(B \rightarrow RP_3)$, which is then compared with theoretical predictions. However, such an approach is valid only in the narrow width limit, $\Gamma_R \rightarrow 0$. In other words, one should have instead

$$\Gamma(B \rightarrow RP_3 \rightarrow P_1P_2P_3)_{\Gamma_R \rightarrow 0} = \Gamma(B \rightarrow RP_3)\mathcal{B}(R \rightarrow P_1P_2), \quad (1.2)$$

where we have assumed that both $\Gamma(B \rightarrow RP_3)$ and $\mathcal{B}(R \rightarrow P_1P_2)$ are not affected by the NWA. In other words, while taking the $\Gamma(R \rightarrow P_1P_2) \rightarrow 0$ limit, the branching fraction of $R \rightarrow P_1P_2$ is assumed to remain intact. For the case when R has a finite-width, Eq. (1.1) does not hold. Moreover, theoretical predictions of $\mathcal{B}(B \rightarrow RP_3)$ are normally calculated under the assumption that the both final-state particles are stable (i.e., $\Gamma_R, \Gamma_{P_3} \rightarrow 0$). Therefore, the question is how one should extract $\mathcal{B}(B \rightarrow RP_3)$ from the experimental measurement of the partial rate of $B \rightarrow RP_3 \rightarrow P_1P_2P_3$ and make a meaningful comparison with its theoretical predictions.

Let us define a quantity ¹

$$\eta_R \equiv \frac{\Gamma(B \rightarrow RP_3 \rightarrow P_1P_2P_3)_{\Gamma_R \rightarrow 0}}{\Gamma(B \rightarrow RP_3 \rightarrow P_1P_2P_3)} = \frac{\Gamma(B \rightarrow RP_3)\mathcal{B}(R \rightarrow P_1P_2)}{\Gamma(B \rightarrow RP_3 \rightarrow P_1P_2P_3)} = 1 + \delta, \quad (1.3)$$

so that the deviation of η_R from unity measures the degree of departure from the NWA when the width is finite. It is naively expected that the correction δ will be of order Γ_R/m_R . The quantity η_R extrapolates the three-body decay from the physical width to the zero width. It is calculable theoretically but depends on the line shape of the resonance and the approach of describing weak hadronic decays such as QCD factorization (QCDF), perturbative QCD and soft collinear effective theory. After taking into account the finite-width effect η_R from the resonance, the branching fraction of the quasi-two-body decay reads

$$\mathcal{B}(B \rightarrow RP_3) = \eta_R \frac{\mathcal{B}(B \rightarrow RP_3 \rightarrow P_1P_2P_3)_{\text{expt}}}{\mathcal{B}(R \rightarrow P_1P_2)_{\text{expt}}}. \quad (1.4)$$

Note that $\mathcal{B}(B \rightarrow RP_3)$ on the left-hand side of the above formula is the branching fraction under the assumption that both R and P_3 are stable and thus have zero decay width. Therefore, it is suitable for a comparison with theoretical calculations.

¹ For later convenience, our definition of η_R here is inverse to the one defined in [1]. A similar (but inversely) quantity $\mathcal{W}_R^{(\ell)} = \Gamma_R^{(\ell)}/\Gamma_{R,\text{NWL}}^{(\ell)}$ was also considered in [2], where $\Gamma_R^{(\ell)}$ is the partial-wave decay rate integrated in a region around a resonance and $\Gamma_{R,\text{NWL}}^{(\ell)}$ denotes $\Gamma_R^{(\ell)}$ in the narrow width limit.

In the literature, such as the Particle Data Group [3], the branching fraction of the quasi-two-body decay is often inferred from Eq. (1.4) by setting η_R equal to unity. While this is justified for narrow-width resonances, it is not for the broad ones. For example, $\Gamma_\rho/m_\rho = 0.192$ for the ρ vector meson, $\Gamma_{f_2}/m_{f_2} = 0.146$ for the $f_2(1270)$ tensor meson, $\Gamma_\sigma/m_\sigma \sim \mathcal{O}(1)$ for the $\sigma/f_0(500)$ scalar meson, and $\Gamma_{K_2^*}/m_{K_2^*} \approx 0.189$ for the $K_2^*(1430)$ tensor meson. For these resonances, finite-width effects seem to be important and cannot be neglected. We shall see in this work that the deviation of η_R from unity does not always follow the guideline from the magnitude of Γ_R/m_R .

It is worth mentioning that the finite-width effects play an essential role in charmed meson decays [1, 4]. There exist some modes, *e.g.*, $D^0 \rightarrow \rho(1700)^+ K^-$, $D^0 \rightarrow K^*(1410)^- K^+$ which are not allowed kinematically can proceed through the finite-width effects.

In this work, we will calculate the parameter η_R within the framework of QCDF for various resonances and use these examples to highlight the importance of finite-width effects. First, we need to check the NWA relation Eq. (1.2) both analytically and numerically. Once this is done, it is straightforward to compute η_R .

In the experimental analysis of $B \rightarrow RP_3 \rightarrow P_1 P_2 P_3$ decays, it is customary to parameterize the amplitude as $A(m_{12}, m_{23}) = cF(m_{12}, m_{23})$, where the strong dynamics is described by the function F that parameterizes the intermediate resonant processes, while the information of weak interactions is encoded in the complex coefficient c which is obtained by fitting to the measured Dalitz plot. The function F can be further parameterized in terms of a resonance line shape, an angular dependence and Blatt-Weisskopf barrier factors. Using the experimental parameterization of $F(m_{12}, m_{23})$, we can also compute the ratio of the three-body decay rate without and with the finite-width effects of the resonance, which we shall refer to as η_R^{EXPP} . Obviously, η_R^{EXPP} is independent of c . On the contrary, the weak decay amplitude of $B \rightarrow R(m_{12})P_3$ generally has some dependence on m_{12} in QCDF calculations. Hence, η_R^{QCDF} is different from η_R^{EXPP} in general. It will be instructive to compare them to gain more insight to the underlying mechanism.

Although it is straightforward to estimate the parameter η_R in a theoretical framework by computing the decay rates of the quasi-two-body decay and the corresponding three-body decay, we shall develop a general framework for the study of η_R . We will show that η_R can be expressed in terms of a normalized differential decay rate. It turns out that η_R is nothing but the value of the normalized differential decay rate evaluated at the contributing resonance. Not only is the calculation significantly simplified, the underlying physics also becomes more transparent. Finally, we note in passing that while we focus on three-body B meson decays in this paper to elucidate our point and explain the cause, our finding generally applies to all quasi-two-body decays.

The layout of the present paper is as follows. In Sec. II, we present a general framework for the study of the parameter η_R and show that it can be obtained from the normalized differential decay rate. The experimental analysis of $B \rightarrow RP_3 \rightarrow P_1 P_2 P_3$ decays relies on a parameterization of the involved strong dynamics. This is discussed in detail in Sec. III. We then proceed to evaluate η_R^{QCDF} within the framework of QCDF in Sec. IV for some selected processes mediated by tensor, vector and scalar resonances, and compare them with η_R^{EXPP} determined from the experimental parameterization. We discuss our findings in Sec. V. Sec. VI comes to our conclusions. A more concise version of this work has been presented in [5].

II. GENERAL FRAMEWORK

In this section, we discuss how η_R can be determined from a normalized differential decay rate. We start by considering the simpler case where the mediating resonance is a scalar meson, and show that the result reduces to the usual one in the NWA. We then generalize our discussions to resonances of arbitrary spin, and derive an important relation between η_R and the normalized differential decay rate evaluated at the resonance mass. Two examples of the $\rho(770)$ and $\sigma/f_0(500)$ resonances are presented at the end of the section.

A. Scalar intermediate states

We first consider the case that R is a scalar resonance for simplicity. The three-body $B \rightarrow RP_3 \rightarrow P_1P_2P_3$ decay amplitude has the following form:

$$A(m_{12}, m_{23}) = \frac{\mathcal{M}[B \rightarrow R(m_{12})P_3]\mathcal{M}[R(m_{12}) \rightarrow P_1P_2]}{(m_{12}^2 - m_R^2) + im_R\Gamma_R}, \quad (2.1)$$

where $\mathcal{M}[B \rightarrow R(m_{12})P_3]$ and $\mathcal{M}[R(m_{12}) \rightarrow P_1P_2]$ are weak and strong decay amplitudes of $B \rightarrow R(m_{12})P_3$ and $R(m_{12}) \rightarrow P_1P_2$ decays, respectively, and $m_{ij}^2 \equiv p_{ij}^2 \equiv (p_i + p_j)^2$. Note that at the resonance, we have

$$i\sqrt{\pi m_R\Gamma_R} A(m_R, m_{23}) = \mathcal{M}[B \rightarrow R(m_R)P_3] \frac{\mathcal{M}[R(m_R) \rightarrow P_1P_2]}{\sqrt{m_R\Gamma_R/\pi}}, \quad (2.2)$$

which contains the critical information of the physical $B \rightarrow RP_3$ and $R \rightarrow P_1P_2$ decay amplitudes.

Using the standard formulas [3], the three-body differential decay rate at the resonance is given by

$$\frac{D\Gamma(m_R^2)}{dm_{12}^2} = \frac{1}{(2\pi)^3} \frac{1}{32m_B^3} \int |A(m_R, m_{23})|^2 dm_{23}^2, \quad (2.3)$$

or, equivalently,

$$\frac{D\Gamma(m_R^2)}{dm_{12}^2} = \frac{1}{(2\pi)^5} \frac{1}{32m_R m_B^2} \int |A(m_R, m_{23})|^2 |\vec{p}_1| |\vec{p}_3| d\Omega_1 d\Omega_3, \quad (2.4)$$

where $|\vec{p}_1|$ and Ω_1 are evaluated in the R rest frame. With the help of Eq. (2.2), the above equation can be rewritten as

$$\begin{aligned} \pi m_R \Gamma_R \frac{D\Gamma(m_R^2)}{dm_{12}^2} &= \frac{1}{32\pi^2} \int |\mathcal{M}[B \rightarrow R(m_R)P_3]|^2 \frac{|\vec{p}_3|}{m_B^2} d\Omega_3 \\ &\quad \times \left(\frac{1}{32\pi^2} \int |\mathcal{M}[R(m_R) \rightarrow P_1P_2]|^2 \frac{|\vec{p}_1|}{m_R^2} d\Omega_1 \right) / \Gamma_R, \\ &= \Gamma(B \rightarrow RP_3) \mathcal{B}(R \rightarrow P_1P_2). \end{aligned} \quad (2.5)$$

Hence, we obtain

$$\begin{aligned} \Gamma(B \rightarrow RP_3) \mathcal{B}(R \rightarrow P_1P_2) &= \pi m_R \Gamma_R \frac{D\Gamma(m_R^2)}{dm_{12}^2} \\ &= \frac{\pi m_R \Gamma_R}{(2\pi)^3} \frac{1}{32m_B^3} \int_{(m_{23}^2)_{\min.}(m_R)}^{(m_{23}^2)_{\max.}(m_R)} |A(m_R, m_{23})|^2 dm_{23}^2. \end{aligned} \quad (2.6)$$

Consequently, Eqs. (2.6) and (1.3) imply that η_R is related to the normalized differential rate,

$$\eta_R = \frac{\pi m_R \Gamma_R \frac{D \Gamma(m_R^2)}{dm_{12}^2}}{\int \frac{D \Gamma(m_{12}^2)}{dm_{12}^2} dm_{12}^2} = \pi m_R \Gamma_R \frac{\int |A(m_R, m_{23})|^2 dm_{23}^2}{\int |A(m_{12}, m_{23})|^2 dm_{12}^2 dm_{23}^2}. \quad (2.7)$$

With the help of the following identity ²

$$\lim_{\Gamma_R \rightarrow 0} \frac{m_R \Gamma_R / \pi}{(m_{12}^2 - m_R^2)^2 + m_R^2 \Gamma_R^2} = \delta(m_{12}^2 - m_R^2), \quad (2.8)$$

one can readily verify that η_R given in the above equation approaches unity in the narrow width limit, reproducing the well-known result of Eq. (1.2).

B. General case

Although Eqs. (2.6) and (2.7) are derived for the case of a scalar resonance, they can be generalized to a more generic case, where the resonance particle has spin J . Instead of Eq. (2.1), the general amplitude has the following expression:

$$A(m_{12}, m_{23}) = \mathcal{M}(m_{12}, m_{12}) R_J(m_{12}) \mathcal{T}_J(m_{12}, m_{23}), \quad (2.9)$$

where $\mathcal{M}(m_{12}, m_{12})$ is a regular function containing the information of $B \rightarrow R(m_{12})P_3$ weak decay and $R(m_{12}) \rightarrow P_1 P_2$ strong decay, R_J describes the line shape of the resonance and \mathcal{T}_J encodes the angular dependence. Resonant contributions are commonly depicted by the relativistic Breit-Wigner (BW) line shape,

$$R_J^{\text{BW}}(m_{12}) = \frac{1}{(m_{12}^2 - m_R^2) + im_R \Gamma_R(m_{12})}. \quad (2.10)$$

In general, the mass-dependent width is expressed as

$$\Gamma_R(m_{12}) = \Gamma_R^0 \left(\frac{q}{q_0} \right)^{2J+1} \frac{m_R X_J^2(q)}{m_{12} X_J^2(q_0)}, \quad (2.11)$$

where $q = |\vec{p}_1| = |\vec{p}_2|$ is the center-of-mass (c.m.) momentum in the rest frame of the resonance R , q_0 is the value of q when m_{12} is equal to the pole mass m_R , and X_J is a Blatt-Weisskopf barrier factor given by

$$X_0(z) = 1, \quad X_1(z) = \sqrt{\frac{1}{(z r_{\text{BW}})^2 + 1}}, \quad X_2(z) = \sqrt{\frac{1}{(z r_{\text{BW}})^4 + 3(z r_{\text{BW}})^2 + 9}}, \quad (2.12)$$

with $r_{\text{BW}} \approx 4.0 \text{ GeV}^{-1}$. In Eq. (2.11), Γ_R^0 is the nominal total width of R with $\Gamma_R^0 = \Gamma_R(m_R)$. One advantage of using the energy-dependent decay width is that $\Gamma_R(m_{12})$ vanishes when m_{12} is below the $m_1 + m_2$ threshold (see the expression of q in Eq. (3.9) below). Hence, the factor q^{2L+1} with L being the orbital angular momentum between R and P_3 guarantees the correct threshold behavior.

² This follows from the formula: $\lim_{\epsilon \rightarrow 0} \frac{\epsilon}{\epsilon^2 + x^2} = \pi \delta(x)$.

The rapid growth of this factor for angular momenta $> L$ is compensated at higher energies by the Blatt-Weisskopf barrier factors [3].

From Eqs. (3.8), (3.10), (4.46), (4.61) and (4.102) below, we find that the angular distribution term \mathcal{T}_J in Eq. (2.9) at the resonance is governed by the Legendre polynomial $P_J(\cos \theta)$, where θ is the angle between \vec{p}_1 and \vec{p}_3 measured in the rest frame of the resonance (see also [6]). Explicitly, we have

$$P_0(\cos \theta) = 1, \quad P_1(\cos \theta) = \cos \theta, \quad P_2(\cos \theta) = \frac{1}{2}(-1 + 3 \cos^2 \theta), \quad (2.13)$$

and

$$\mathcal{T}_0(m_R, m_{23}) = 1, \quad \mathcal{T}_1(m_R, m_{23}) \propto \cos \theta, \quad \mathcal{T}_2(m_R, m_{23}) \propto 1 - 3 \cos^2 \theta. \quad (2.14)$$

Note that $\mathcal{T}_0(m_{12}, m_{23}) = 1$ throughout the entire phase space. This means that the strong and weak amplitudes can always be separated for the scalar case, as shown in Eq. (2.1).

Instead of Eq. (2.2), the general amplitude *at the resonance* takes the form

$$i\sqrt{\pi m_R \Gamma_R^0} A(m_R, m_{23}) = \sum_{\lambda} \mathcal{M}_{\lambda}[B \rightarrow R(m_R)P_3] \frac{\mathcal{M}_{\lambda}[R(m_R) \rightarrow P_1P_2]}{\sqrt{m_R \Gamma_R^0/\pi}}, \quad (2.15)$$

where λ is the helicity of the resonance R . Such a relation is expectable because there is a propagator of the resonance R in the amplitude $A(m_{12}, m_{23})$ and its denominator reduces to $im_R \Gamma_R^0$ on the mass shell of m_{12} while its numerator reduces to a polarization sum of the polarization vectors, producing the above structure after contracted with the rest of the amplitude.

From Eq. (2.4) and Eq. (2.15), we have

$$\frac{D\Gamma(m_R^2)}{dm_{12}^2} = \frac{1}{(32\pi^2)^2 \pi m_R (\Gamma_R^0)^2} \int \left| \sum_{\lambda} \mathcal{M}_{\lambda}[B \rightarrow R(m_R)P_3] \mathcal{M}_{\lambda}[R(m_R) \rightarrow P_1P_2] \right|^2 \frac{|\vec{p}_1| |\vec{p}_3|}{m_R^2 m_B^2} d\Omega_3 d\Omega_1, \quad (2.16)$$

where $|\vec{p}_1|$ and Ω_1 are evaluated in the R rest frame. In this frame the sum over helicities in the amplitude can be replaced by the sum over spins. Consequently, $\mathcal{M}_{\lambda}[B \rightarrow R(m_R)P_3]$ and $\mathcal{M}_{\lambda}[R(m_R) \rightarrow P_1P_2]$ are proportional to $Y_{J\lambda}^*(\Omega_3)$ and $Y_{J\lambda}(\Omega_1)$, respectively.³ As a cross check, we note that Eq. (2.14) can be reproduced by using the well-known addition theorem of spherical harmonics, $(2J+1)P_J(\cos \theta) = 4\pi \sum_{\lambda} Y_{J\lambda}^*(\Omega_3) Y_{J\lambda}(\Omega_1)$. Alternatively, we can start from Eq. (2.14) and make use of the addition theorem to obtain the $\sum_{\lambda} Y_{J\lambda}^*(\Omega_3) Y_{J\lambda}(\Omega_1)$ factor.

We now see that the interference terms in Eq. (2.16) from different helicities (or spins) vanish after the angular integrations. As a result, we obtain

$$\begin{aligned} \pi m_R \Gamma_R \frac{D\Gamma(m_R^2)}{dm_{12}^2} &= \frac{1}{32\pi^2} \sum_{\lambda} \int |\mathcal{M}_{\lambda}[B \rightarrow R(m_R)P_3]|^2 \frac{|\vec{p}_3|}{m_B^2} d\Omega_3 \\ &\quad \times \left(\frac{1}{32\pi^2} \int |\mathcal{M}_{\lambda}[R(m_R) \rightarrow P_1P_2]|^2 \frac{|\vec{p}_1|}{m_R^2} d\Omega_1 \right) / \Gamma_R^0 \\ &= \Gamma(B \rightarrow RP_3) \mathcal{B}(R \rightarrow P_1P_2), \end{aligned} \quad (2.17)$$

³ For example, in the $J = 1$ case and at the resonance, $\mathcal{M}_{\lambda}[B \rightarrow V(m_R)P_3]$ is proportional to $p_B \cdot \epsilon^*(p_{12}, \lambda)$, while $\mathcal{M}_{\lambda}[V(m_R) \rightarrow P_1P_2]$ is proportional to $\epsilon(p_{12}, \lambda) \cdot (p_1 - p_2)$. See also Eq. (3.8) below. It can be easily seen that in the V rest frame, these terms provide the $Y_{1\lambda}^*(\Omega_3)$ and $Y_{1\lambda}(\Omega_1)$ factors, respectively.

where we have made use of the fact that the branching fraction $\mathcal{B}(R \rightarrow P_1 P_2)$ is independent of the helicity (or spin) in the last step. The above equation agrees with Eq. (2.6), and consequently Eq. (2.7) follows.

Eq. (2.7) can be easily generalized to the case with identical particles in the final state. Let P_2 and P_3 be identical particles so that the decay amplitude reads $\mathcal{M} = A(m_{12}, m_{23}) + A(m_{13}, m_{23})$, giving

$$\eta_R = \pi m_R \Gamma_R \frac{2 \int |A(m_R, m_{23})|^2 dm_{23}^2}{\int |A(m_{12}, m_{23}) + A(m_{13}, m_{23})|^2 dm_{12}^2 dm_{23}^2}. \quad (2.18)$$

Furthermore, from Eqs. (2.8) and (2.9), we see that in the narrow width limit, the amplitude squared takes the form

$$|A(m_{12}, m_{23})|_{\Gamma_R^0 \rightarrow 0}^2 = \pi m_R \Gamma_R^0 \delta(m_{12}^2 - m_R^2) |A(m_R, m_{23})|^2. \quad (2.19)$$

Substituting this into Eq. (2.7), we obtain $\eta_R = 1$ in the limit of zero width, hence reproducing the well known result in Eq. (1.2).

In this work, we will consider $A(m_{12}, m_{23})$ using the experimental parameterization (EXPP) and the QCDF calculation and compute η_R^{EXPP} and η_R^{QCDF} , respectively. In the latter case, we shall see that in the narrow width limit, the weak interaction part of the amplitude does reduce to the QCDF amplitude of the $B \rightarrow RP_3$ decay. We will also show explicitly the validity of the factorization relation in the zero width limit for several selected examples of three-body decays involving tensor, vector and scalar mediating resonances.

C. η_R and the normalized differential rate

As suggested by Eq. (2.7), η_R can be expressed in terms of the normalized differential rate,

$$\eta_R = \pi m_R \Gamma_R \frac{d\tilde{\Gamma}(m_R^2)}{dm_{12}^2} = \frac{1}{2} \pi \Gamma_R \frac{d\tilde{\Gamma}(m_R)}{dm_{12}}, \quad (2.20)$$

where we have defined

$$\frac{d\tilde{\Gamma}(m_{12}^2)}{dm_{12}^2} \equiv \frac{D \Gamma(m_{12}^2)}{dm_{12}^2} \Big/ \int \frac{D \Gamma(m_{12}^2)}{dm_{12}^2} dm_{12}^2. \quad (2.21)$$

Hence η_R is determined by the value of the normalized differential rate at the resonance. It should be noted that as the normalized differential rate is always positive and normalized to 1 after integration, the value of $d\tilde{\Gamma}(m_R)/dm_{12}$ is anticorrelated with $d\tilde{\Gamma}(m_{12})/dm_{12}$ elsewhere. Hence, it is the shape of the (normalized) differential rate that matters in the determination of η_R .

The above point can be made more precise. When $\Gamma_R/m_R \ll 1$, we expect that the normalized differential rate around the resonance is reasonably well described as

$$\left. \frac{d\tilde{\Gamma}(m_{12}^2)}{dm_{12}^2} \right|_{m_{12}^2 \simeq m_R^2} \simeq \frac{m_R^2 \Gamma_R^2}{(m_{12}^2 - m_R^2)^2 + m_R^2 \Gamma_R^2} \frac{d\tilde{\Gamma}(m_R^2)}{dm_{12}^2}. \quad (2.22)$$

It is straightforward to show that as a result, Eq. (2.20) can be approximated by

$$\eta_R \simeq \frac{\pi}{2 \tan^{-1} 2} \int_{(m_R - \Gamma_R)^2}^{(m_R + \Gamma_R)^2} \frac{d\tilde{\Gamma}(m_{12}^2)}{dm_{12}^2} dm_{12}^2, \quad (2.23)$$

or, equivalently,

$$\eta_R \simeq \frac{\pi}{2 \tan^{-1} 2} \int_{m_R - \Gamma_R}^{m_R + \Gamma_R} \frac{d\tilde{\Gamma}(m_{12})}{dm_{12}} dm_{12} = \frac{\pi}{2 \tan^{-1} 2} \left(1 - \int_{\text{elsewhere}} \frac{d\tilde{\Gamma}(m_{12})}{dm_{12}} dm_{12} \right). \quad (2.24)$$

It becomes clear that η_R represents the fraction of rates around the resonance and is anticorrelated with the fraction of rates off the resonance.

The EXPP and the QCDF approaches may have different shapes in the differential rates, resulting in different η_R 's, *i.e.*, $\eta_R^{\text{EXPP}} \neq \eta_R^{\text{QCDF}}$ in general. The two-body rate reported by experiments should be corrected using $\eta_R = \eta_R^{\text{EXPP}}$ in Eq. (1.4), as the data are extracted using the experimental parameterization. On the other hand, the experimental parameterization on normalized differential rates should be compared with the theoretical predictions from QCDF calculation as the latter takes into account the energy dependence of weak interaction amplitudes. As we shall show in Sec. V.A, the usual experimental parameterization ignores the momentum dependence in weak dynamics and would lead to incorrect extraction of quasi-two-body decay rates in the case of broad resonances, as contrasted with the estimates using the QCDF approach.

D. Formula of η_R in the case of the Gounaris-Sakurai line shape

A popular choice for describing the broad $\rho(770)$ resonance is the Gounaris-Sakurai (GS) model [7]. It was employed by both BaBar [8] and LHCb [9, 10] Collaborations in their analyses of the $\rho(770)$ resonance in the $B^- \rightarrow \pi^+ \pi^- \pi^-$ decay. The GS line shape for $\rho(770)$ is given by

$$T_\rho^{\text{GS}}(s) = \frac{1 + D\Gamma_\rho^0/m_\rho}{s - m_\rho^2 - f(s) + im_\rho\Gamma_\rho(s)}, \quad (2.25)$$

where

$$\Gamma_\rho(s) = \Gamma_\rho^0 \left(\frac{q}{q_0} \right)^3 \frac{m_\rho X_1^2(q)}{\sqrt{s} X_1^2(q_0)}, \quad (2.26)$$

the Blatt-Weisskopf barrier factor is given in Eq. (2.12), Γ_ρ^0 is the nominal total ρ width with $\Gamma_\rho^0 = \Gamma_\rho(m_\rho^2)$. The quantities q and q_0 are already introduced before in Sec. II.A. In this model, the real part of the pion-pion scattering amplitude with an intermediate ρ exchange calculated from the dispersion relation is taken into account by the $f(s)$ term in the propagator of $T_\rho^{\text{GS}}(s)$. Unitarity far from the pole mass is thus ensured. Explicitly,

$$f(s) = \Gamma_\rho^0 \frac{m_\rho^2}{q_0^3} \left[q^2 [h(\sqrt{s}) - h(m_\rho)] + (m_\rho^2 - s) q_0^2 \frac{dh}{ds} \Big|_{m_\rho} \right], \quad (2.27)$$

and

$$h(s) = \frac{2}{\pi} \frac{q}{\sqrt{s}} \ln \left(\frac{\sqrt{s} + 2q}{2m_\pi} \right), \quad \frac{dh}{ds} \Big|_{m_\rho} = h(m_\rho) \left[\frac{1}{8q_0^2} - \frac{1}{2m_\rho^2} \right] + \frac{1}{2\pi m_\rho^2}. \quad (2.28)$$

The constant parameter D is given by

$$D = \frac{3}{\pi} \frac{m_\pi^2}{q_0^2} \ln \left(\frac{m_\rho + 2q_0}{2m_\pi} \right) + \frac{m_\rho}{2\pi q_0} - \frac{m_\pi^2 m_\rho}{\pi q_0^3}. \quad (2.29)$$

The $(1 + D\Gamma_\rho^0/m_\rho)$ factor in Eq. (2.25) will modify the relation in Eq. (2.15) into

$$i \frac{\sqrt{\pi m_R \Gamma_R^0}}{(1 + D\Gamma_\rho^0/m_\rho)} A^{\text{GS}}(m_\rho, m_{23}) = \sum_\lambda \mathcal{M}_\lambda[B \rightarrow \rho(m_R)P_3] \frac{\mathcal{M}_\lambda[\rho(m_R) \rightarrow P_1 P_2]}{\sqrt{m_R \Gamma_R^0/\pi}} \quad (2.30)$$

instead. It can be easily seen that Eqs. (2.6), (2.7) and (2.20) all need to be corrected by the factor of $1/(1 + D\Gamma_\rho^0/m_\rho)^2$ accordingly. More explicitly, Eqs. (2.7) and (2.20) should be replaced by

$$\eta_\rho^{\text{GS}} = \frac{\pi m_\rho \Gamma_\rho}{(1 + D\Gamma_\rho^0/m_\rho)^2} \frac{\int |A(m_\rho, m_{23})|^2 dm_{23}^2}{\int |A(m_{12}, m_{23})|^2 dm_{12}^2 dm_{23}^2} \quad (2.31)$$

and

$$\eta_\rho^{\text{GS}} = \frac{\pi m_\rho \Gamma_\rho^0}{(1 + D\Gamma_\rho^0/m_\rho)^2} \frac{d\tilde{\Gamma}(m_\rho^2)}{dm_{12}^2} = \frac{\pi \Gamma_\rho^0}{2(1 + D\Gamma_\rho^0/m_\rho)^2} \frac{d\tilde{\Gamma}(m_\rho)}{dm_{12}}, \quad (2.32)$$

respectively.

E. Formula of η_R in the case of the $\sigma/f_0(500)$ resonance

As stressed in [11], the scalar resonance $\sigma/f_0(500)$ is very broad and cannot be described by the usual Breit-Wigner line shape. The partial wave amplitude does not resemble a Breit-Wigner shape with a clear peak and a simultaneous steep rise in the phase. The mass and width of the σ resonance are identified from the associated pole position $\sqrt{s_\sigma}$ of the partial wave amplitude in the second Riemann sheet as $\sqrt{s_\sigma} = m_\sigma - i\Gamma_\sigma/2$ [11]. Hence, we shall follow the LHCb Collaboration [10] to use a simple pole description

$$T_\sigma(s) = \frac{1}{s - s_\sigma} = \frac{1}{s - m_\sigma^2 + \Gamma_\sigma^2(s)/4 + im_\sigma \Gamma_\sigma(s)}, \quad (2.33)$$

with

$$\Gamma_\sigma(s) = \Gamma_\sigma^0 \left(\frac{q}{q_0} \right) \frac{m_\sigma}{\sqrt{s}}, \quad (2.34)$$

and $\Gamma_\sigma(m_\sigma^2) = \Gamma_\sigma^0$.

The factor of $1/[(\Gamma_\sigma^0)^2/4 + im_\sigma \Gamma_\sigma^0] = (im_\sigma \Gamma_\sigma^0)^{-1} (1 - i\Gamma_\sigma^0/4m_\sigma)^{-1}$ in Eq. (2.33) at the resonance will modify the relation in Eq. (2.15) into

$$\left(1 - i \frac{\Gamma_\sigma^0}{4m_\sigma} \right) i \sqrt{\pi m_R \Gamma_R^0} A(m_\sigma, m_{23}) = \sum_\lambda \mathcal{M}_\lambda[B \rightarrow \sigma(m_R)P_3] \frac{\mathcal{M}_\lambda[\sigma(m_R) \rightarrow P_1 P_2]}{\sqrt{m_R \Gamma_R^0/\pi}} \quad (2.35)$$

instead. It can be easily seen that Eqs. (2.6), (2.7) and (2.20) all need to be corrected by the factor of $r_\sigma \equiv [1 + (\Gamma_\sigma^0/4m_\sigma)^2]$ accordingly. More explicitly, Eqs. (2.7) and (2.20) should be replaced by

$$\eta_\sigma = \pi r_\sigma m_\sigma \Gamma_\sigma \frac{\int |A(m_\sigma, m_{23})|^2 dm_{23}^2}{\int |A(m_{12}, m_{23})|^2 dm_{12}^2 dm_{23}^2} \quad (2.36)$$

and

$$\eta_\sigma = \pi r_\sigma m_\sigma \Gamma_\sigma^0 \frac{d\tilde{\Gamma}(m_\sigma^2)}{dm_{12}^2} = \frac{\pi r_\sigma \Gamma_\sigma^0}{2} \frac{d\tilde{\Gamma}(m_\sigma)}{dm_{12}}, \quad (2.37)$$

respectively.

III. DIFFERENTIAL RATES AND η_R^{EXPP} USING THE EXPERIMENTAL PARAMETERIZATION

The following parameterization of the decay amplitude is widely used in the experimental studies of $B \rightarrow RP_3 \rightarrow P_1 P_2 P_3$ decays (see, for example, [12]):

$$A(m_{12}, m_{23}) = cF(m_{12}, m_{23}) = cR_J(m_{12}) \times X_J(p_3) \times X_J(p_1) \times T_J(m_{12}, m_{23}), \quad (3.1)$$

where R_J describes the line shape of the resonance introduced before in Eq. (2.10), X_J is the Blatt-Weisskopf barrier form factor as defined in Eq. (2.12) with both p_1 and p_3 evaluated in the $R(m_{12})$ rest frame, $T_J(m_{12}, m_{23})$ is an angular distribution term given by [6],

$$\begin{aligned} T_0(m_{12}, m_{23}) &= 1, \\ T_1(m_{12}, m_{23}) &= m_{23}^2 - m_{13}^2 + \frac{(m_B^2 - m_3^2)(m_1^2 - m_2^2)}{m_{12}^2}, \\ T_2(m_{12}, m_{23}) &= \left(m_{23}^2 - m_{13}^2 + \frac{(m_B^2 - m_3^2)(m_1^2 - m_2^2)}{m_{12}^2} \right)^2 \\ &\quad - \frac{1}{3} \left(m_{12}^2 - 2m_B^2 - 2m_3^2 + \frac{(m_B^2 - m_3^2)^2}{m_{12}^2} \right) \\ &\quad \times \left(m_{12}^2 - 2m_1^2 - 2m_2^2 + \frac{(m_1^2 - m_2^2)^2}{m_{12}^2} \right), \end{aligned} \quad (3.2)$$

and c is an unknown complex coefficient to be fitted to the data. Basically the information of weak decay amplitude is included in c . However, it is assumed to be a constant and have no dependence on the energy or momentum of the decay products.

The quantities $\Gamma(B \rightarrow RP_3)\mathcal{B}(R \rightarrow P_1 P_2)$ and η_R^{EXPP} can be obtained by using Eqs. (2.6) and (2.7) as

$$\begin{aligned} \Gamma(B \rightarrow RP_3)\mathcal{B}(R \rightarrow P_1 P_2) &= \frac{|c|^2}{8\pi^2 m_R \Gamma_R} \frac{1}{32m_B^3} \int_{(m_{23}^2)_{\min.}(m_R)}^{(m_{23}^2)_{\max.}(m_R)} (|X_J(p_3)|^2 |X_J(p_1)|^2)_{m_{12} \rightarrow m_R} \\ &\quad \times |T_J(m_R, m_{23})|^2 dm_{23}^2, \end{aligned} \quad (3.3)$$

and

$$\eta_R^{\text{EXPP}} = \frac{\pi}{m_R \Gamma_R} \frac{\int_{(m_{23}^2)_{\min.}(m_R)}^{(m_{23}^2)_{\max.}(m_R)} (|X_J(p_3)|^2 |X_J(p_1)|^2)_{m_{12} \rightarrow m_R} \times |T_J(m_R, m_{23})|^2 dm_{23}^2}{\int |R_J(m_{12}) \times X_J(p_3) \times X_J(p_1) \times T_J(m_{12}, m_{23})|^2 dm_{12}^2 dm_{23}^2}. \quad (3.4)$$

Note that being a constant, the factor c in $A(m_{12}, m_{23})$ is canceled out between the numerator and the denominator in η_R^{EXPP} . One can readily verify that η_R^{EXPP} approaches unity in the narrow width limit by virtue of Eq. (2.8).

We can express η_R^{EXPP} in terms of the normalized differential rate,

$$\eta_R^{\text{EXPP}} = \pi m_R \Gamma_R \frac{d\tilde{\Gamma}(m_R^2)}{dm_{12}^2} = \frac{1}{2} \pi \Gamma_R \frac{d\tilde{\Gamma}(m_R)}{dm_{12}}, \quad (3.5)$$

with

$$\frac{d\tilde{\Gamma}(m_{12}^2)}{dm_{12}^2} = \frac{|R_J(m_{12})|^2 \int |X_J(p_3) \times X_J(p_1) \times T_J(m_R, m_{23})|^2 dm_{23}^2}{\int |R_J(m_{12}) \times X_J(p_3) \times X_J(p_1) \times T_J(m_{12}, m_{23})|^2 dm_{12}^2 dm_{23}^2}. \quad (3.6)$$

In the case that P_2 and P_3 are identical particles, we shall use Eq. (2.18) to obtain η_R^{EXPP} , giving

$$\eta_R^{\text{EXPP}} = \frac{2\pi \int_{(m_{23}^2)_{\min.}(m_R)}^{(m_{23}^2)_{\max.}(m_R)} (|X_J(p_3)|^2 |X_J(p_1)|^2)_{m_{12} \rightarrow m_R} \times |T_J(m_R, m_{23})|^2 dm_{23}^2}{m_R \Gamma_R \int |R_J(m_{12}) \times X_J(p_3) \times X_J(p_1) \times T_J(m_{12}, m_{23}) + (2 \leftrightarrow 3)|^2 dm_{12}^2 dm_{23}^2}. \quad (3.7)$$

Note that when the Gounaris-Sakurai line shape is used in place of R_J , we should use Eqs. (2.31) and (2.32), instead of Eq. (3.5), while Eqs. (3.4) and (3.6) are still valid. For the case of the σ resonance, we should use Eqs. (2.36) and (2.37).

In the case of narrow width, it is legitimate to use a complex constant c to represent the weak dynamics. As noted previously, it is the shape of the entire normalized differential rate that matters in determining η_R . Hence, in the case of finite-width, the momentum dependence in the weak amplitude will play some role.

There are some subtleties in the angular terms. Note that Eq. (3.2) was obtained with transversality conditions, $p_{12}^\mu \epsilon_\mu = 0$ and $p_{12}^\mu p_{12}^\nu \epsilon_{\mu\nu} = 0$, enforced for $J = 1, 2$, [6]

$$\begin{aligned} T_1(m_{12}, m_{23}) &= \sum_\lambda (p_B + p_3)_\mu \epsilon^{*\mu}(p_{12}, \lambda) \epsilon^\nu(p_{12}, \lambda) (p_1 - p_2)_\nu \\ &= -2\vec{p}_1 \cdot \vec{p}_3 = -2q|\vec{p}_3| \cos \theta, \\ T_2(m_{12}, m_{23}) &= \sum_\lambda (p_B + p_3)_\mu (p_B + p_3)_\nu \epsilon^{*\mu\nu}(p_{12}, \lambda) \epsilon^{\alpha\beta}(p_{12}, \lambda) (p_1 - p_2)_\alpha (p_1 - p_2)_\beta \\ &= \frac{4}{3} [3(\vec{p}_1 \cdot \vec{p}_3)^2 - (|\vec{p}_1||\vec{p}_3|)^2] = \frac{4}{3} q^2 |\vec{p}_3|^2 (3 \cos^2 \theta - 1), \end{aligned} \quad (3.8)$$

where ϵ^μ and $\epsilon^{\mu\nu}$ are the polarization vector and tensor, respectively, and

$$\begin{aligned} q = |\vec{p}_1| = |\vec{p}_2| &= \frac{\sqrt{[m_{12}^2 - (m_1 + m_2)^2][m_{12}^2 - (m_1 - m_2)^2]}}{2m_{12}}, \\ |\vec{p}_3| &= \left(\frac{(m_B^2 - m_3^2 - m_{12}^2)^2}{4m_{12}^2} - m_3^2 \right)^{1/2}, \end{aligned} \quad (3.9)$$

with $q = |\vec{p}_{1,2}|$ and $|\vec{p}_3|$ being the momenta of $P_{1,2}$ and P_3 in the $R(m_{12})$ rest frame, respectively.⁴ Note that in Eq. (3.8), the factor contracted with $(p_B + p_3)$ comes from the $B \rightarrow R(m_{12})P$ weak decay amplitude, while the one contracted with $(p_1 - p_2)$ comes from the $R(m_{12}) \rightarrow P_1P_2$ strong decay amplitude. To obtain the $\cos\theta$ dependence, it is useful to recall $\sum_\lambda \epsilon_\mu^*(p_{12}, \lambda)\epsilon_\nu(p_{12}, \lambda) = g_\mu^i g_\nu^j \delta_{ij}$ in the rest frame of $R(m_{12})$.

Alternatively, using the standard expressions of vector and tensor propagators, which are contracted with the $B \rightarrow R(m_{12})P$ and the $R(m_{12}) \rightarrow P_1P_2$ parts, we expect the angular terms to take the following forms,

$$\begin{aligned} T'_1(m_{12}, m_{23}) &= m_{23}^2 - m_{13}^2 + \frac{(m_B^2 - m_3^2)(m_1^2 - m_2^2)}{m_R^2}, \\ T'_2(m_{12}, m_{23}) &= \left(m_{23}^2 - m_{13}^2 + \frac{(m_B^2 - m_3^2)(m_1^2 - m_2^2)}{m_R^2} \right)^2 \\ &\quad - \frac{1}{3} \left(m_{12}^2 - 2m_B^2 - 2m_3^2 + \frac{(m_B^2 - m_3^2)^2}{m_R^2} \right) \\ &\quad \times \left(m_{12}^2 - 2m_1^2 - 2m_2^2 + \frac{(m_1^2 - m_2^2)^2}{m_R^2} \right). \end{aligned} \quad (3.10)$$

The transversality condition, however, is not imposed on the above equations as the denominators become m_R^2 instead of m_{12}^2 . In general, these T'_J cannot be expressed as Eq. (3.8) except on the mass shell of p_{12} , where these two angular terms coincide, *i.e.*, $T'_J(m_R, m_{23}) = T_J(m_R, m_{23})$. In the case of a vector resonance, except for modes with the intermediate resonance decaying to daughters of different masses, these two angular terms are identical throughout the entire phase space. We will also consider the case where the transversality condition is not imposed.

IV. ANALYSIS IN THE QCD FACTORIZATION APPROACH

In this section we will evaluate the decay amplitudes of $B \rightarrow RP_3$ and $B \rightarrow RP_3 \rightarrow P_1P_2P_3$ within the framework of QCD factorization [13, 14]. For the latter, its general amplitude has the expression

$$\begin{aligned} A(B \rightarrow RP_3 \rightarrow P_1P_2P_3) &\equiv A(m_{12}, m_{23}) \\ &= g^{R \rightarrow P_1P_2} F(s_{12}, m_R) \tilde{A}(B \rightarrow R(m_{12})P_3) R_J(m_{12}) \mathcal{T}_J(m_{12}, m_{23}), \end{aligned} \quad (4.1)$$

where $g^{R \rightarrow P_1P_2}$ is the strong coupling constant associated with the strong decay $R(m_{12}) \rightarrow P_1P_2$, $F(s, m_R)$ is a form factor to be introduced later (see Eq. (4.20) below), R_J is the resonance line shape, and \mathcal{T}_J is the angular distribution function. In this work, we find

$$\mathcal{T}_0 = 1, \quad \mathcal{T}_1 = 2q \cos\theta, \quad \mathcal{T}_2 = \frac{q^2}{\sqrt{6}}(1 - 3\cos^2\theta), \quad (4.2)$$

⁴ Note that $|\vec{p}_3|$ is related to \tilde{p}_c through the relation $\tilde{p}_c = (m_{12}/m_B)|\vec{p}_3|$, where \tilde{p}_c is the c.m. momentum of P_3 or $R(m_{12})$ in the B rest frame. This relation can be easily verified using the conservation of momentum.

where θ is the angle between \vec{p}_1 and \vec{p}_3 measured in the rest frame of the resonance and q is given before in Eq. (3.9). In Eq. (4.1), the weak decay amplitude $\tilde{A}(B \rightarrow R(m_{12})P_3)$ will be reduced to the QCDF amplitude $A(B \rightarrow R(m_R)P_3)$ when $m_{12} \rightarrow m_R$.

Taking the relativistic Breit-Wigner line shape Eq. (2.10), it follows from Eqs. (2.2) and (2.4) that

$$\begin{aligned} \frac{D\Gamma(m_R^2)}{dm_{12}^2} &= \frac{1}{(2\pi)^5} \frac{1}{32m_R m_B^2} \int |A(m_R, m_{23})|^2 |\vec{p}_1| |\vec{p}_3| d\Omega_1 d\Omega_3, \\ &= \frac{1}{\pi m_R \Gamma_R^2} \left(\frac{1}{32\pi^2} \int |A(B \rightarrow R(m_R)P_3)|^2 \frac{|\vec{p}_3|}{m_B^2} d\Omega_3 \right) \left(\frac{1}{32\pi^2} \int |g^{R \rightarrow P_1 P_2} \mathcal{T}_J|^2 \frac{|\vec{p}_1|}{m_R^2} d\Omega_1 \right), \\ &= \frac{1}{\pi m_R \Gamma_R} \Gamma(B \rightarrow RP_3) \mathcal{B}(R \rightarrow P_1 P_2). \end{aligned} \quad (4.3)$$

Indeed, it is straightforward to show that the partial rate of $R(m_R) \rightarrow P_1 P_2$ given by

$$\Gamma(R \rightarrow P_1 P_2) = \frac{1}{32\pi^2} \int |g^{R \rightarrow P_1 P_2} \mathcal{T}_J|^2 \frac{q_0}{m_R^2} d\Omega_1 \quad (4.4)$$

has the following expressions (see also Eq. (2.39) of [17])

$$\Gamma_{S \rightarrow P_1 P_2} = \frac{q_0}{8\pi m_S^2} g_{S \rightarrow P_1 P_2}^2, \quad \Gamma_{V \rightarrow P_1 P_2} = \frac{q_0^3}{6\pi m_V^2} g_{V \rightarrow P_1 P_2}^2, \quad \Gamma_{T \rightarrow P_1 P_2} = \frac{q_0^5}{60\pi m_T^2} g_{T \rightarrow P_1 P_2}^2, \quad (4.5)$$

for different types of resonances. Therefore, the decay rate of $B \rightarrow R(m_R)P_3$ can be related to the differential rate of $B \rightarrow RP_3 \rightarrow P_1 P_2 P_3$ at the resonance. This means that η_R can be obtained from the normalized differential rate as shown in Eq. (2.7) or (2.20).

Most of the input parameters employed in this section such as decay constants, form factors, CKM matrix elements can be found in Appendix A of [17].

A. Tensor resonances

We begin with the tensor resonances and consider the three-body decay processes: $B^- \rightarrow f_2(1270)\pi^- \rightarrow \pi^+\pi^-\pi^-$ and $B^- \rightarrow \bar{K}_2^{*0}(1430)\pi^- \rightarrow K^-\pi^+\pi^-$. Since the decay widths of $f_2(1270)$ and $K_2^*(1430)$ are around 187 and 109 MeV, respectively, it is naively expected that the deviation of η_{f_2} from unity is larger than that of $\eta_{K_2^*}$ in both QCDF and EXPP schemes. We shall see below that this is not respected in the QCDF scheme and barely holds in the EXPP scheme.

1. $f_2(1270)$

$B^- \rightarrow f_2(1270)\pi^-$ decay in QCDF

Consider the process $B^- \rightarrow f_2(1270)\pi^- \rightarrow \pi^+\pi^-\pi^-$. In QCDF, the amplitude of the quasi-two-

body decay $B^- \rightarrow f_2(1270)\pi^-$ is given by [15]

$$\begin{aligned}
A(B^- \rightarrow f_2(1270)\pi^-) &= \frac{G_F}{2} \sum_{p=u,c} \lambda_p^{(d)} \\
&\times \left\{ \left[a_1 \delta_{pu} + a_4^p + a_{10}^p - (a_6^p + a_8^p) r_\chi^\pi + \beta_2^p \delta_{pu} + \beta_3^p + \beta_{3,\text{EW}}^p \right]_{f_2\pi} X^{(Bf_2,\pi)} \right. \\
&\quad + \left[a_2 \delta_{pu} + 2(a_3^p + a_5^p) + a_4^p + r_\chi^{f_2} a_6^p + \frac{1}{2}(a_7^p + a_9^p) - \frac{1}{2}(a_{10}^p + r_\chi^{f_2} a_8^p) \right. \\
&\quad \left. \left. + \beta_2^p \delta_{pu} + \beta_3^p + \beta_{3,\text{EW}}^p \right]_{\pi f_2} X^{(B\pi,f_2)} \right\}, \tag{4.6}
\end{aligned}$$

where $\lambda_p^{(d)} \equiv V_{pb} V_{pd}^*$, and

$$X^{(Bf_2,\pi)} = 2f_\pi A_0^{Bf_2} (m_\pi^2) \frac{m_{f_2}}{m_B} \epsilon^{*\mu\nu}(0) p_{B\mu} p_{B\nu}, \quad X^{(B\pi,f_2)} = 2f_{f_2} m_B p_c F_1^{B\pi}(m_{f_2}^2), \tag{4.7}$$

with p_c being the c.m. momentum of either f_2 or π^- in the B rest frame. The chiral factors r_χ^π and $r_\chi^{f_2}$ in Eq. (4.6) are given by

$$r_\chi^\pi(\mu) = \frac{2m_\pi^2}{m_b(\mu)(m_u + m_d)(\mu)}, \quad r_\chi^{f_2}(\mu) = \frac{2m_{f_2}}{m_b(\mu)} \frac{f_{f_2}^\perp(\mu)}{f_{f_2}}. \tag{4.8}$$

For the definition of the scale-dependent decay constants f_{f_2} and $f_{f_2}^\perp$, see, for example, Ref. [15]. The coefficients β_i^p describe weak annihilation contributions to the decay. The order of the arguments in the $a_i^p(M_1 M_2)$ and $\beta_i^p(M_1 M_2)$ coefficients is dictated by the subscript $M_1 M_2$ given in Eq. (4.6).

In Eq. (4.7), $X^{(Bf_2,\pi)}$ is factorizable and given by $\langle \pi | J^\mu | 0 \rangle \langle f_2 | J'_\mu | B^- \rangle$, while $X^{(B\pi,f_2)}$ is a non-factorizable amplitude as the factorizable one $\langle f_2 | J^\mu | 0 \rangle \langle \pi^- | J'_\mu | B^- \rangle$ vanishes owing to the fact that the tensor meson cannot be produced through the $V - A$ current. Nevertheless, beyond the factorization approximation, contributions proportional to the decay constant f_{f_2} can be produced from vertex, penguin and spectator-scattering corrections [15]. Therefore, when the strong coupling α_s is turned off, the nonfactorizable contributions vanish accordingly.

The factorizable amplitude $X^{(Bf_2,\pi)}$ can be further simplified by working in the B rest frame and assuming that f_2 (π) moves along the $-z$ (z) axis [15]. In this case, $p_B^\mu = (m_B, 0, 0, 0)$ and $\epsilon^{*\mu\nu}(0) = \sqrt{2/3} \epsilon^{*\mu}(0) \epsilon^{*\nu}(0)$ with $\epsilon^{*\mu}(0) = (p_c, 0, 0, E_{f_2})^\mu / m_{f_2}$ and, consequently,

$$X^{(Bf_2,\pi)} = 2\sqrt{\frac{2}{3}} f_\pi \frac{m_B}{m_{f_2}} p_c^2 A_0^{Bf_2}(m_\pi^2). \tag{4.9}$$

Three-body decay $B^- \rightarrow f_2(1270)\pi^- \rightarrow \pi^+\pi^-\pi^-$

As shown in [17], the decay amplitude $\mathcal{A}_{f_2(1270)} \equiv A(B^- \rightarrow \pi^- f_2(1270) \rightarrow \pi^-(p_1)\pi^+(p_2)\pi^-(p_3))$ evaluated in the factorization approach⁵ arises from the matrix element $\langle \pi^+(p_2)\pi^-(p_3) | (\bar{u}b) | B^- \rangle^{f_2} \langle \pi^-(p_1) | (\bar{d}u) | 0 \rangle$, where $(\bar{q}_1 q_2) \equiv \bar{q}_1 \gamma_\mu (1 - \gamma_5) q_2$ and the superscript f_2

⁵ The study of charmless three-body B decays in the factorization approach can be found in [17–20] and references therein.

denotes the contribution from the f_2 resonance to the matrix element $\langle \pi^+(p_2)\pi^-(p_3)|(\bar{u}b)|B^- \rangle$. We shall use the relativistic Breit-Wigner line shape to describe the distribution of $f_2(1270)$:

$$T_{f_2}^{\text{BW}}(s) = \frac{1}{s - m_{f_2}^2 + im_{f_2}\Gamma_{f_2}(s)}, \quad (4.10)$$

with

$$\Gamma_{f_2}(s) = \Gamma_{f_2}^0 \left(\frac{q}{q_0} \right)^5 \frac{m_{f_2}}{\sqrt{s}} \frac{X_2^2(q)}{X_2^2(q_0)}, \quad (4.11)$$

where the quantities q , q_0 , X_2 and Γ_T^0 are already introduced before in Eq. (2.11). One advantage of using the energy-dependent decay width is that $\Gamma_{f_2}(s)$ will vanish when s goes below the 2π threshold.

Consequently,

$$\begin{aligned} & \langle \pi^+(p_2)\pi^-(p_3)|(\bar{u}b)|B^- \rangle^{f_2} \langle \pi^-(p_1)|(\bar{d}u)|0 \rangle \\ &= \langle \pi^+(p_2)\pi^-(p_3)|f_2 \rangle T_{f_2}^{\text{BW}}(s_{23}) \langle f_2|(\bar{u}b)|B^- \rangle \langle \pi^-(p_1)|(\bar{d}u)|0 \rangle \\ &= \sum_{\lambda} \varepsilon^{*\mu\nu}(\lambda) p_{2\mu} p_{3\nu} g^{f_2 \rightarrow \pi^+\pi^-} T_{f_2}^{\text{BW}}(s_{23}) \frac{2m_{f_2}}{m_B} f_{\pi} A_0^{Bf_2}(m_{\pi}^2) \varepsilon_{\alpha\beta}(\lambda) p_B^{\alpha} p_1^{\beta} \\ &= \frac{2m_{f_2}}{m_B} g^{f_2 \rightarrow \pi^+\pi^-} f_{\pi} A_0^{Bf_2}(m_{\pi}^2) T_{f_2}^{\text{BW}}(s_{23}) \left[\frac{1}{3} (|\vec{p}_1||\vec{p}_2|^2 - (\vec{p}_1 \cdot \vec{p}_2)^2) \right], \end{aligned} \quad (4.12)$$

where we have followed [21] for the definition of the $B \rightarrow T$ transition form factors⁶ and employed the relation [6, 23]

$$\sum_{\lambda} \varepsilon^{*\mu\nu}(\lambda) \varepsilon_{\alpha\beta}(\lambda) p_{2\mu} p_{3\nu} p_B^{\alpha} p_1^{\beta} = \frac{1}{3} (|\vec{p}_1||\vec{p}_2|^2 - (\vec{p}_1 \cdot \vec{p}_2)^2), \quad (4.13)$$

with

$$|\vec{p}_1| = \left(\frac{(m_B^2 - m_{\pi}^2 - s_{23})^2}{4s_{23}} - m_{\pi}^2 \right)^{1/2}, \quad |\vec{p}_2| = |\vec{p}_3| = q = \frac{1}{2} \sqrt{s_{23} - 4m_{\pi}^2}. \quad (4.14)$$

Hence, factorization leads to

$$\begin{aligned} \mathcal{A}_{f_2(1270)} &= \frac{1}{\sqrt{2}} \frac{G_F}{\sqrt{2}} \sum_{p=u,c} \lambda_p^{(d)} [a_1 \delta_{pu} + a_4^p + a_{10}^p - (a_6^p + a_8^p) r_{\chi}^{\pi}] \\ &\quad \times \frac{2m_{f_2}}{m_B} g^{f_2 \rightarrow \pi^+\pi^-} f_{\pi} A_0^{Bf_2}(m_{\pi}^2) T_{f_2}^{\text{BW}}(s_{23}) \frac{1}{3} |\vec{p}_1|^2 |\vec{p}_2|^2 (1 - 3 \cos^2 \theta) + (s_{23} \leftrightarrow s_{12}), \end{aligned} \quad (4.15)$$

where the identical particle effect due to the two identical π^- has been taken into account. Comparing with Eq. (4.6), we see that the nonfactorizable contribution characterized by $X^{(B\pi, f_2)}$ and the weak annihilation described by β^p terms are absent in the naïve factorization approach. We shall use the QCDF expression for $B^- \rightarrow f_2(1270)\pi^-$ and write

$$\mathcal{A}_{f_2(1270)} = g^{f_2 \rightarrow \pi^+\pi^-} T_{f_2}^{\text{BW}}(s_{23}) \frac{q^2}{\sqrt{6}} (1 - 3 \cos^2 \theta) \tilde{A}(B^- \rightarrow f_2(m_{23})\pi^-) + (s_{23} \leftrightarrow s_{12}), \quad (4.16)$$

⁶ The $B \rightarrow T$ transition form factors defined in [21] and [15] differ by a factor of i . We shall use the former as they are consistent with the normalization of $B \rightarrow S$ transition given in [22].

with

$$\begin{aligned} \tilde{A}(B^- \rightarrow f_2(m_{23})\pi^-) &= \frac{G_F}{2} \sum_{p=u,c} \lambda_p^{(d)} \frac{m_{f_2}^2}{s_{23}} \left\{ \left[a_1 \delta_{pu} + a_4^p + \cdots + \beta_{3,\text{EW}}^p \right]_{f_2\pi} \tilde{X}^{(Bf_2,\pi)} \right. \\ &\quad \left. + \left[a_2 \delta_{pu} + 2(a_3^p + a_5^p) + \cdots + \beta_{3,\text{EW}}^p \right]_{\pi f_2} \tilde{X}^{(B\pi,f_2)} \right\}, \end{aligned} \quad (4.17)$$

where

$$\tilde{X}^{(Bf_2,\pi)} = 2\sqrt{\frac{2}{3}} f_\pi \frac{m_B}{m_{f_2}} \tilde{p}_c^2 A_0^{Bf_2}(m_\pi^2), \quad \tilde{X}^{(B\pi,f_2)} = 2f_{f_2} m_B \tilde{p}_c F_1^{B\pi}(s_{23}), \quad (4.18)$$

and

$$\tilde{p}_c = \left(\frac{(m_B^2 - m_\pi^2 - s_{23})^2}{4m_B^2} - m_\pi^2 \right)^{1/2}. \quad (4.19)$$

It is easily seen that $\tilde{A}(B^- \rightarrow f_2(m_{23})\pi^-)$ is reduced to the QCDF amplitude $A(B^- \rightarrow f_2\pi^-)$ given in Eq. (4.6) when $m_{23} \rightarrow m_{f_2}$.

Before proceeding, we would like to address an issue. The strong coupling constant $|g^{f_2(1270) \rightarrow \pi^+\pi^-}| = 18.56 \text{ GeV}^{-1}$ extracted from the measured $f_2(1270)$ width (see Eq. (4.27) below) is for the physical $f_2(1270)$. When f_2 is off the mass shell, especially when s_{23} is approaching the upper bound of $(m_B - m_\pi)^2$, it is necessary to account for the off-shell effect. For this purpose, we shall follow [24] to introduce a form factor $F(s, m_R)$ parameterized as ⁷

$$F(s, m_R) = \left(\frac{\Lambda^2 + m_R^2}{\Lambda^2 + s} \right)^n, \quad (4.20)$$

with the cutoff Λ not far from the resonance,

$$\Lambda = m_R + \beta \Lambda_{\text{QCD}}, \quad (4.21)$$

where the parameter β is expected to be of order unity. We shall use $n = 1$, $\Lambda_{\text{QCD}} = 250 \text{ MeV}$ and $\beta = 1.0 \pm 0.2$ in subsequent calculations.

Finally, the decay rate is given by

$$\begin{aligned} &\Gamma(B^- \rightarrow f_2\pi^- \rightarrow \pi^+\pi^-\pi^-) \\ &= \frac{1}{2} \frac{1}{(2\pi)^3 32m_B^3} \int_{(m_\pi+m_\pi)^2}^{(m_B-m_\pi)^2} ds_{23} \int_{(s_{12})_{\min}}^{(s_{12})_{\max}} ds_{12} |\mathcal{A}_{f_2}|^2 \\ &= \frac{1}{2} \frac{1}{(2\pi)^3 32m_B^3} \int_{(m_\pi+m_\pi)^2}^{(m_B-m_\pi)^2} ds_{23} \int_{(s_{12})_{\min}}^{(s_{12})_{\max}} ds_{12} \left\{ \frac{|g^{f_2 \rightarrow \pi^+\pi^-}|^2 F(s_{23}, m_{f_2})^2}{(s_{23} - m_{f_2}^2)^2 + m_{f_2}^2 \Gamma_{f_2}^2(s_{23})} \right. \\ &\quad \left. \times \frac{q^4}{6} (1 - 3\cos^2\theta)^2 \left| \tilde{A}(B^- \rightarrow f_2\pi^-) \right|^2 + (s_{23} \leftrightarrow s_{12}) + \text{interference terms} \right\}, \end{aligned} \quad (4.22)$$

where the factor of 1/2 accounts for the identical-particle effect. Note that $\cos\theta$ can be expressed as in terms of s_{12} and s_{23} :

$$\cos\theta = a(s_{23})s_{12} + b(s_{23}), \quad (4.23)$$

⁷ Note that the form factor $F(t, m)$ used in [24] is for the t -channel off-shell effect.

with [25]

$$\begin{aligned} a(s) &= \frac{1}{(s - 4m_\pi^2)^{1/2} \left(\frac{(m_B^2 - m_\pi^2 - s)^2}{4s} - m_\pi^2 \right)^{1/2}}, \\ b(s) &= -\frac{m_B^2 + 3m_\pi^2 - s}{2(s - 4m_\pi^2)^{1/2} \left(\frac{(m_B^2 - m_\pi^2 - s)^2}{4s} - m_\pi^2 \right)^{1/2}}. \end{aligned} \quad (4.24)$$

It follows that $(s_{12})_{\min} = -(1+b)/a$ and $(s_{12})_{\max} = (1-b)/a$. It is straightforward to show that

$$\int_{(s_{12})_{\min}}^{(s_{12})_{\max}} ds_{12} (1 - 3 \cos^2 \theta)^2 = \frac{8}{5a} = \frac{16}{5} \frac{m_B}{\sqrt{s_{23}}} q \tilde{p}_c. \quad (4.25)$$

In the narrow width limit, we have

$$\frac{m_{f_2} \Gamma_{f_2}(s)}{(s - m_{f_2}^2)^2 + m_{f_2}^2 \Gamma_{f_2}^2(s)} \xrightarrow{\Gamma_{f_2} \rightarrow 0} \pi \delta(s - m_{f_2}^2). \quad (4.26)$$

Under the NWA, $|g^{f_2 \rightarrow \pi^+ \pi^-}|^2 / \Gamma_{f_2}$ is finite as it is proportional to the branching fraction $\mathcal{B}(f_2 \rightarrow \pi^+ \pi^-)$. Due to the Dirac δ -function in the above equation, we have $s_{23} \rightarrow m_{f_2}^2$ in the zero width limit. As a result, $\tilde{p}_c \rightarrow p_c$, $q \rightarrow q_0$, $\tilde{X}^{(Bf_2, \pi)} \rightarrow X^{(Bf_2, \pi)}$, $\tilde{X}^{(B\pi, f_2)} \rightarrow X^{(B\pi, f_2)}$ and $\tilde{A}(B^- \rightarrow f_2 \pi^-) \rightarrow A(B^- \rightarrow f_2 \pi^-)$. Likewise, the second term in Eq. (4.22) with the replacement $s_{23} \leftrightarrow s_{12}$ has a similar expression. However, the interference term vanishes in the NWA due to different δ -functions. Using

$$\Gamma_{f_2 \rightarrow \pi^+ \pi^-} = \frac{q_0^5}{60\pi m_{f_2}^2} |g^{f_2 \rightarrow \pi^+ \pi^-}|^2, \quad \Gamma_{B^- \rightarrow f_2 \pi^-} = \frac{p_c}{8\pi m_B^2} |A(B^- \rightarrow f_2 \pi^-)|^2, \quad (4.27)$$

we are led to the desired factorization relation:

$$\Gamma(B^- \rightarrow f_2 \pi^- \rightarrow \pi^+ \pi^- \pi^-) \xrightarrow{\Gamma_{f_2} \rightarrow 0} \Gamma(B^- \rightarrow f_2 \pi^-) \mathcal{B}(f_2 \rightarrow \pi^+ \pi^-). \quad (4.28)$$

Numerical results

To compute $B^- \rightarrow f_2 \pi^-$ and the three-body decay $B^- \rightarrow f_2 \pi^- \rightarrow \pi^+ \pi^- \pi^-$, we need to know the values of the flavor operators $a_i^p(M_1, M_2)$. In the QCDF approach, the flavor operators have the expressions [13, 14]

$$a_i^p(M_1, M_2) = \left(c_i + \frac{c_{i\pm 1}}{N_c} \right) N_i(M_2) + \frac{c_{i\pm 1}}{N_c} \frac{C_F \alpha_s}{4\pi} \left[V_i(M_2) + \frac{4\pi^2}{N_c} H_i(M_1 M_2) \right] + P_i^p(M_2), \quad (4.29)$$

where $i = 1, \dots, 10$, the upper (lower) sign is for odd (even) i , c_i are the Wilson coefficients, $C_F = (N_c^2 - 1)/(2N_c)$ with $N_c = 3$, M_2 is the emitted meson, and M_1 shares the same spectator quark with the B meson. The detailed expressions for the vertex corrections $V_i(M_2)$, hard spectator interactions $H_i(M_1 M_2)$ and penguin contractions $P_i^p(M_2)$ for $M_1 M_2 = TP$ and PT can be found in [15]. Note that the parameters $N_i(M)$ in Eq. (4.29) vanish if M is a tensor meson; otherwise, it is equal to one. Therefore, the coefficient $a_2(\pi f_2)$ appearing in Eq. (4.6) vanishes when the strong coupling α_s is turned off. We see from Table I that $a_i^p(f_2 P)$ and $a_i^p(P f_2)$ can be quite different.

It is known that power corrections in QCDF always involve troublesome endpoint divergences. For example, the annihilation amplitude has endpoint divergences even at twist-2 level, and the hard

spectator scattering diagram at twist-3 order is power suppressed and possesses soft and collinear divergences arising from the soft spectator quark. Since the treatment of endpoint divergences is model-dependent, we shall follow [13] to model the endpoint divergence $X \equiv \int_0^1 dx/\bar{x}$ in the annihilation and hard spectator scattering diagrams as

$$X_A = \ln\left(\frac{m_B}{\Lambda_h}\right) (1 + \rho_A e^{i\phi_A}), \quad X_H = \ln\left(\frac{m_B}{\Lambda_h}\right) (1 + \rho_H e^{i\phi_H}), \quad (4.30)$$

with Λ_h being a typical hadronic scale of 0.5 GeV. In this work we use

$$\rho_A^{TP} = \rho_A^{PT} = 0.7, \quad \phi_A^{TP} = \phi_A^{PT} = -30^\circ, \quad (4.31)$$

leading to

$$\begin{aligned} \beta_2^p(f_2\pi) &= 0.023 - 0.010i, & (\beta_3^p + \beta_{3,\text{EW}}^p)(f_2\pi) &= -0.047 + 0.053i, \\ \beta_2^p(\pi f_2) &= -0.033 + 0.018i, & (\beta_3^p + \beta_{3,\text{EW}}^p)(\pi f_2) &= -0.050 + 0.047i, \end{aligned} \quad (4.32)$$

for both $p = u$ and c .

Following [15], we obtain the branching fraction and CP asymmetry for $B^- \rightarrow f_2(1270)\pi^-$ as

$$\begin{aligned} \mathcal{B}(B^- \rightarrow f_2(1270)\pi^-)_{\text{QCDF}} &= (2.65_{-1.22}^{+1.29}) \times 10^{-6}, \\ A_{CP}(B^- \rightarrow f_2(1270)\pi^-)_{\text{QCDF}} &= (46.7_{-62.5}^{+32.6})\%, \end{aligned} \quad (4.33)$$

where the decay constants $f_{f_2} = 102 \pm 6$ MeV and $f_{f_2}^\perp = 117 \pm 25$ MeV both at $\mu = 1$ GeV [26], the form factors $A_0^{B f_2(1270)}(0) = 0.13 \pm 0.02$, derived from large energy effective theory (see Table II of [15]), and

$$F_1^{B\pi}(q^2) = \frac{0.26 \pm 0.03}{1 - \frac{q^2}{m_{B^*}^2}} \left(1 + \frac{0.64 \frac{q^2}{m_{B^*}^2}}{1 - 0.40 \frac{q^2}{m_B^2}} \right) \quad (4.34)$$

have been used. The theoretical errors correspond to the uncertainties due to the variation of Gegenbauer moments, decay constants, quark masses, form factors, the λ_B parameter for the B meson wave function and the power-correction parameters $\rho_{A,H}$, $\phi_{A,H}$ (see [15] for details), all added in quadrature. In the narrow width limit, we find the central values

$$\begin{aligned} \mathcal{B}(B^- \rightarrow f_2(1270)\pi^- \rightarrow \pi^+\pi^-\pi^-)_{\Gamma_{f_2 \rightarrow 0}} &= 1.485 \times 10^{-6}, \\ A_{CP}(B^- \rightarrow f_2(1270)\pi^- \rightarrow \pi^+\pi^-\pi^-)_{\Gamma_{f_2 \rightarrow 0}} &= 46.23\%. \end{aligned} \quad (4.35)$$

Since $\mathcal{B}(f_2(1270) \rightarrow \pi^+\pi^-) = (0.842_{-0.009}^{+0.029}) \times \frac{2}{3}$, it is easily seen that the factorization relation Eq. (4.28) is indeed numerically valid in the narrow width limit.

For the finite-width $\Gamma_{f_2}^0 = 186.7_{-2.5}^{+2.2}$ MeV [3], we find

$$\begin{aligned} \mathcal{B}(B^- \rightarrow f_2(1270)\pi^- \rightarrow \pi^+\pi^-\pi^-) &= (1.48_{-0.37}^{+0.42}) \times 10^{-6} \quad [(1.52_{-0.38}^{+0.43}) \times 10^{-6}], \\ A_{CP}(B^- \rightarrow f_2(1270)\pi^- \rightarrow \pi^+\pi^-\pi^-) &= (44.56_{-0.39}^{+0.41})\% \quad [(47.20_{-0.43}^{+0.45})\%], \end{aligned} \quad (4.36)$$

where the values in square parentheses are obtained with the form factor $F(s, m_{f_2})$ being set as unity. They are in agreement with the recent LHCb measurements [9, 10]

$$\begin{aligned} \mathcal{B}(B^- \rightarrow f_2(1270)\pi^- \rightarrow \pi^+\pi^-\pi^-)_{\text{LHCb}} &= (1.37 \pm 0.26) \times 10^{-6}, \\ A_{CP}(B^- \rightarrow f_2(1270)\pi^- \rightarrow \pi^+\pi^-\pi^-)_{\text{LHCb}} &= (46.8 \pm 7.7)\%, \end{aligned} \quad (4.37)$$

TABLE I: Numerical values of the flavor operators $a_i^p(M_1 M_2)$ for $M_1 M_2 = f_2(1270)\pi$ and $\pi f_2(1270)$ at the scale $\mu = \bar{m}_b(\bar{m}_b) = 4.18$ GeV.

a_i^p	$f_2\pi$	πf_2	a_i^p	$f_2\pi$	πf_2
a_1	$1.011 + 0.014i$	$-0.035 + 0.014i$	a_6^c	$-0.053 - 0.005i$	$(6.3 + 1.6i)10^{-3}$
a_2	$0.123 - 0.080i$	$0.133 - 0.078i$	a_7	$(-0.2 + 3.4i)10^{-5}$	$(9.5 - 3.4i)10^{-5}$
a_3	$0.0014 + 0.0027i$	$-0.006 + 0.003i$	a_8^u	$(3.6 - 1.0i)10^{-4}$	$(-2.1 + 0.1i)10^{-5}$
a_4^u	$-0.027 - 0.014i$	$0.0064 - 0.0016i$	a_8^c	$(3.4 - 0.5i)10^{-4}$	$(3.3 + 1.0i)10^{-5}$
a_4^c	$-0.032 - 0.006i$	$0.0091 + 0.0064i$	a_9	$(-9.1 - 0.1i)10^{-3}$	$(3.0 - 1.2i)10^{-4}$
a_5	$0.0009 - 0.0031i$	$-0.008 + 0.003i$	a_{10}^u	$(-8.2 + 6.2i)10^{-4}$	$(-9.6 + 7.0i)10^{-4}$
a_6^u	$-0.050 - 0.014i$	$-(3.52 + 0.02i)10^{-3}$	a_{10}^c	$(-8.5 + 6.7i)10^{-4}$	$(-9.4 + 7.5i)10^{-4}$

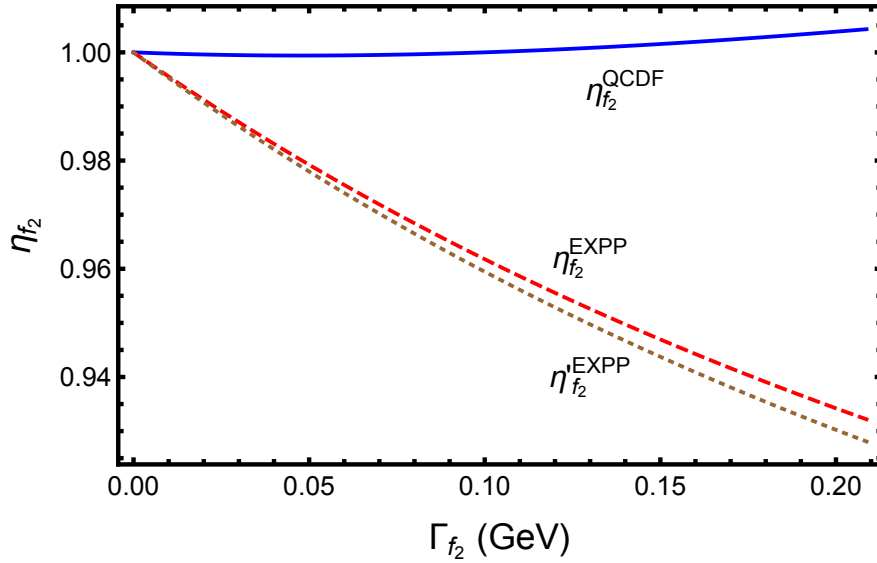


FIG. 1: The parameter η_{f_2} as a function of the $f_2(1270)$ width, where the solid curve is derived from the QCDF calculation and the dashed (dotted) curve from the experimental parameterization (EXPP) with (without) the transversality condition imposed.

and consistent with the earlier BaBar measurements [8]

$$\begin{aligned}
 \mathcal{B}(B^- \rightarrow f_2(1270)\pi^- \rightarrow \pi^+\pi^-\pi^-)_{\text{BaBar}} &= (0.9 \pm 0.2_{-0.1}^{+0.3}) \times 10^{-6}, \\
 A_{CP}(B^- \rightarrow f_2(1270)\pi^- \rightarrow \pi^+\pi^-\pi^-)_{\text{BaBar}} &= (41 \pm 25_{-15}^{+18})\%.
 \end{aligned}
 \tag{4.38}$$

Notice that a large CP asymmetry in the $f_2(1270)$ component was firmly established by the LHCb Collaboration.

We are now in the position to compute the parameter $\eta_{f_2(1270)}$ defined in Eq. (1.3)

$$\eta_{f_2} = \frac{\Gamma(B^- \rightarrow f_2(1270)\pi^-)\mathcal{B}(f_2(1270) \rightarrow \pi^+\pi^-)}{\Gamma(B^- \rightarrow f_2(1270)\pi^- \rightarrow \pi^+\pi^-\pi^-)}.
 \tag{4.39}$$

From Eqs. (4.33) and (4.36) we find

$$\eta_{f_2(1270)}^{\text{QCDF}} = 1.003_{-0.002}^{+0.001} \quad (0.9743 \pm 0.0003). \quad (4.40)$$

Since the theoretical uncertainties in the numerator and denominator essentially cancel out, the errors on η_{f_2} mainly arise from the uncertainties in β and the f_2 width. As discussed in Sec. II, η_R can be expressed in terms of the normalized differential rate. In general, the calculation done in this way is simpler. From Eqs. (2.18) and (4.16) we obtain the same result for $\eta_{f_2}^{\text{QCDF}}$. The dependence of the parameter η_{f_2} on the width Γ_{f_2} is plotted as the solid blue curve in Fig. 1. It is somewhat surprising that the deviation of $\eta_{f_2}^{\text{QCDF}}$ from unity is very tiny, even though Γ_{f_2}/m_{f_2} is about 0.146.

The parameter $\eta_{f_2}^{\text{EXPP}}$ is calculated using Eq. (2.18) together with the experimental parameterization, Eq. (3.1) for $A(m_{12}, m_{23})$. Its dependence on the $f_2(1270)$ width is depicted by the dashed red curve in Fig. 1. At the resonance, we obtain

$$\eta_{f_2(1270)}^{\text{EXPP}} = 0.937_{-0.005}^{+0.006}. \quad (4.41)$$

We see that the the physical with $\Gamma_{f_2}^0 = 186.7_{-2.5}^{+2.2}$ MeV, the results in the QCDF and EXPP schemes differ by about 7%.

2. $K_2^*(1430)$

We next turn to the $B^- \rightarrow \bar{K}_2^{*0}(1430)\pi^- \rightarrow K^-\pi^+\pi^-$ decay. The QCDF amplitude of the quasi-two-body $B^- \rightarrow \bar{K}_2^{*0}(1430)\pi^-$ decay is given by [15]

$$A(B^- \rightarrow \bar{K}_2^{*0}\pi^-) = \frac{G_F}{\sqrt{2}} \sum_{p=u,c} \lambda_p^{(s)} \left[a_4^p + r_\chi^{K_2^*} a_6^p - \frac{1}{2}(a_{10}^p + r_\chi^{K_2^*} a_8) + \beta_2^p \delta_{pu} + \beta_3^p + \beta_{3,\text{EW}}^p \right] X_{\pi K_2^*}^{(B\pi, \bar{K}_2^*)}, \quad (4.42)$$

with $\lambda_p^{(s)} \equiv V_{pb}V_{ps}^*$ and

$$X^{(B\pi, K_2^*)} = 2f_{K_2^*} m_B p_c F_1^{B\pi}(m_{K_2^*}^2). \quad (4.43)$$

Note that this decay proceeds only through nonfactorizable diagrams.

Analogous to the $f_2(1270)$ resonance, the decay amplitude $\mathcal{A}_{K_2^*(1430)} \equiv A(B^- \rightarrow \bar{K}_2^{*0}(1430)\pi^- \rightarrow K^-(p_1)\pi^+(p_2)\pi^-(p_3))$ reads (see the second term of Eq. (4.16))

$$\mathcal{A}_{K_2^*(1430)} = g^{\bar{K}_2^{*0} \rightarrow K^-\pi^+} F(s_{12}, m_{K_2^*}) T_{K_2^*}^{\text{BW}}(s_{12}) \frac{q^2}{\sqrt{6}} (1 - 3 \cos^2 \theta) \tilde{A}(B^- \rightarrow \bar{K}_2^{*0}\pi^-), \quad (4.44)$$

with

$$q = \frac{\sqrt{[s_{12} - (m_K + m_\pi)^2][s_{12} - (m_K - m_\pi)^2]}}{2\sqrt{s_{12}}}, \quad (4.45)$$

and

$$\tilde{A}(B^- \rightarrow \bar{K}_2^{*0}\pi^-) = \frac{G_F}{\sqrt{2}} \sum_{p=u,c} \lambda_p^{(s)} \frac{m_{K_2^*}^2}{s_{12}} \left[a_4^p + \dots + \beta_{3,\text{EW}}^p \right] \tilde{X}_{\pi K_2^*}^{(B\pi, \bar{K}_2^*)}, \quad (4.46)$$

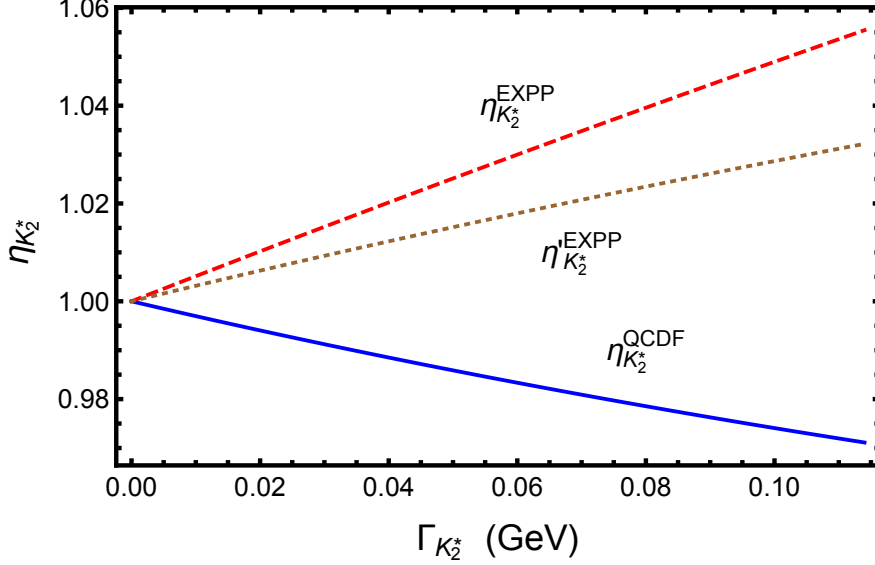


FIG. 2: Same as Fig. 1 for the $\bar{K}_2^*(1430)$ mediating the $B^- \rightarrow K^- \pi^+ \pi^-$ decay.

where $\tilde{X}^{(B\pi, \bar{K}_2^*)}$ has the same expression as $X^{(B\pi, \bar{K}_2^*)}$ except for a replacement of p_c by \tilde{p}_c and $F_1^{B\pi}(m_{K_2^*}^2)$ by $F_1^{B\pi}(s_{12})$. Following the previous case, it is straightforward to show that the factorization relation

$$\Gamma(B^- \rightarrow \bar{K}_2^{*0} \pi^- \rightarrow K^- \pi^+ \pi^-) \xrightarrow{\Gamma_{K_2^* \rightarrow 0}} \Gamma(B^- \rightarrow \bar{K}_2^{*0} \pi^-) \mathcal{B}(\bar{K}_2^{*0} \rightarrow K^- \pi^+), \quad (4.47)$$

holds in the NWA.

In QCDF, we obtain

$$\begin{aligned} \mathcal{B}(B^- \rightarrow \bar{K}_2^{*0}(1430) \pi^-)_{\text{QCDF}} &= (2.60_{-2.53}^{+9.07}) \times 10^{-6}, \\ A_{CP}(B^- \rightarrow \bar{K}_2^{*0}(1430) \pi^-)_{\text{QCDF}} &= (1.72_{-1.95}^{+2.12})\%, \end{aligned} \quad (4.48)$$

where the decay constants $f_{K_2^*} = 118 \pm 5$ MeV and $f_{\bar{K}_2^*}^\perp = 77 \pm 14$ MeV at $\mu = 1$ GeV [26], and the penguin annihilation effects

$$\beta_2^p(\pi K_2^*) = 0.017 + 0.006i, \quad (\beta_3^p + \beta_{3,\text{EW}}^p)(\pi K_2^*) = -0.027 + 0.022i \quad (4.49)$$

have been used. In the narrow width limit, we find that

$$\mathcal{B}(B^- \rightarrow \bar{K}_2^{*0}(1430) \pi^- \rightarrow K^- \pi^+ \pi^-)_{\Gamma_{K_2^* \rightarrow 0}} = 0.864 \times 10^{-6}. \quad (4.50)$$

Since $\mathcal{B}(K_2^{*0}(1430) \rightarrow \pi^+ \pi^-) = (0.499 \pm 0.012) \times \frac{2}{3}$ [3], it is seen that the factorization relation Eq. (4.47) is numerically satisfied.

With the finite-width $\Gamma_{K_2^{*0}}^0 = 109 \pm 5$ MeV, we obtain ⁸

$$\begin{aligned} \mathcal{B}(B^- \rightarrow \bar{K}_2^{*0}(1432) \pi^- \rightarrow K^- \pi^+ \pi^-) &= (0.89_{-0.19}^{+0.22}) \times 10^{-6}, \\ A_{CP}(B^- \rightarrow \bar{K}_2^{*0}(1432) \pi^- \rightarrow K^- \pi^+ \pi^-) &= (1.711 \pm 0.002)\%, \end{aligned} \quad (4.51)$$

⁸ Contrary to the phase space integration in Eq. (4.22) for $B^- \rightarrow f_2 \pi^- \rightarrow \pi + \pi^- \pi^-$, here one should integrate over s_{12} first and then s_{23} owing to a pole structure in $T^{\text{BW}}(s_{12})$ at $s_{12} = m_{K_2^*}^2$.

and

$$\eta_{K_2^*}^{\text{QCDF}} = 0.972 \pm 0.001 \quad (0.715 \pm 0.009). \quad (4.52)$$

As for the $\eta_{K_2^*}$ parameter in the experimental parameterization, we need to consider two possibilities for the angular distribution function: T_2 in Eq. (3.2) imposed with the transversality condition and T_2' in Eq. (3.10) without the transversality condition. We thus find

$$\eta_{K_2^*}^{\text{EXPP}} = 1.053 \pm 0.002, \quad \eta'_{K_2^*}{}^{\text{EXPP}} = 1.031 \pm 0.001. \quad (4.53)$$

Therefore, the transversality condition has little impact on the determination of η_R . The dependence of $\eta_{K_2^*}$ in QCDF and in experimental parameterization is shown in Fig. 2. Experimentally, the BaBar measurement [12] yields

$$\mathcal{B}(B^- \rightarrow \overline{K}_2^{*0}(1430)\pi^- \rightarrow K^- \pi^+ \pi^-)_{\text{expt}} = (1.85_{-0.50}^{+0.73}) \times 10^{-6}. \quad (4.54)$$

Our result of Eq. (4.51) for the branching fraction is consistent with experiment within uncertainties.

Comparing $\eta_{K_2^*}$'s with η_{f_2} 's, it is clear that the proximity of $\eta_{f_2}^{\text{QCDF}}$ to unity in QCDF is unexpected, while the deviation of η_R from unity in the EXPP scenario is barely consistent with the expectation from the ratio of Γ_R/m_R for $R = f_2(1270)$ and $K_2^*(1430)$.

B. Vector mesons

We take the processes $B^- \rightarrow \rho(770)\pi^- \rightarrow \pi^+\pi^-\pi^-$ and $B^- \rightarrow \overline{K}^{*0}(892)\pi^- \rightarrow K^-\pi^+\pi^-$ as examples to illustrate the width effects associated with the vector mesons.⁹ It is known that $\rho(770)$ is much broader than $K^*(892)$. Therefore, it is expected that the former is subject to a larger width effect.

1. $\rho(770)\pi^-$

$B^- \rightarrow \rho^0(770)\pi^- \rightarrow \pi^+\pi^-\pi^-$ decay in QCDF

The decay amplitude of the quasi-two-body decay $B^- \rightarrow \rho^0\pi^-$ in QCDF reads [14]

$$\begin{aligned} A(B^- \rightarrow \rho^0\pi^-) = \frac{G_F}{2} \sum_{p=u,c} \lambda_p^{(d)} \left\{ \left[\delta_{pu}(a_2 - \beta_2) - a_4^p - r_\chi^\rho a_6^p + \frac{3}{2}(a_7^p + a_9^p) + \frac{1}{2}(a_{10}^p + r_\chi^\rho a_8^p) \right. \right. \\ \left. \left. - \beta_3^p - \beta_{3,\text{EW}}^p \right]_{\pi\rho} X^{(B^-\pi,\rho)} + \left[\delta_{pu}(a_1 + \beta_2) + a_4^p - r_\chi^\pi a_6^p + a_{10}^p - r_\chi^\pi a_8^p \right. \right. \\ \left. \left. + \beta_3^p + \beta_{3,\text{EW}}^p \right]_{\rho\pi} X^{(B^-\rho,\pi)} \right\}, \quad (4.55) \end{aligned}$$

with the chiral factor

$$r_\chi^\rho(\mu) = \frac{2m_\rho}{m_b(\mu)} \frac{f_\rho^\perp(\mu)}{f_\rho}, \quad (4.56)$$

⁹ For an early discussion on the decay $B \rightarrow \rho\pi \rightarrow 3\pi$, see [16].

and the factorizable matrix elements

$$X^{(B^-\pi,\rho)} = 2f_\rho m_B p_c F_1^{B\pi}(m_\rho^2), \quad X^{(B^-\rho,\pi)} = 2f_\pi m_B p_c A_0^{B\rho}(m_\pi^2), \quad (4.57)$$

where we have followed [27] for the definitions of $B \rightarrow P$ and $B \rightarrow V$ transition form factors.

The so-called Gounaris-Sakurai model [7] is a popular approach for describing the broad $\rho(770)$ resonance. The line shape is introduced in Eq. (2.25). Note that the GS line shape for $\rho(770)$ was employed by both BaBar [8] and LHCb [9, 10] in their analysis of the $\rho(770)$ resonance in the $B^- \rightarrow \pi^+\pi^-\pi^-$ decay.

For the three-body decay amplitude $\mathcal{A}_{\rho(770)} \equiv A(B^- \rightarrow \rho^0(770)\pi^- \rightarrow \pi^-(p_1)\pi^+(p_2)\pi^-(p_3))$, factorization leads to the expression [17]

$$\begin{aligned} \mathcal{A}_{\rho(770)} = & -\frac{G_F}{2} \sum_{p=u,c} \lambda_p^{(d)} g^{\rho \rightarrow \pi^+\pi^-} F(s_{23}, m_\rho) T_\rho^{\text{GS}}(s_{23})(s_{12} - s_{13}) \\ & \times \left\{ f_\pi \left[m_\rho A_0^{B\rho}(m_\pi^2) + \frac{1}{2} \left(m_B - m_\rho - \frac{m_B^2 - s_{23}}{m_B + m_\rho} \right) A_2^{B\rho}(m_\pi^2) \right] \right. \\ & \times \left[\delta_{pu}(a_1 + \beta_2) + a_4^p - r_\chi^\pi a_6^p + a_{10}^p - r_\chi^\pi a_8^p + \beta_3^p + \beta_{3,\text{EW}}^p \right]_{\rho\pi} + m_\rho f_\rho F_1^{B\pi}(s_{23}) \\ & \times \left. \left[\delta_{pu}(a_2 - \beta_2) - a_4^p - r_\chi^\rho a_6^p + \frac{3}{2}(a_7^p + a_9^p) + \frac{1}{2}(a_{10}^p + r_\chi^\rho a_8^p) - \beta_3^p - \beta_{3,\text{EW}}^p \right]_{\pi\rho} \right\} \\ & + (s_{23} \leftrightarrow s_{12}). \end{aligned} \quad (4.58)$$

Penguin annihilation terms characterized by β_2 , β_3 and $\beta_{3,\text{EW}}$, which are absent in naïve factorization, are included here. Note that

$$s_{12} - s_{13} = -4\vec{p}_1 \cdot \vec{p}_2 = 4\vec{p}_1 \cdot \vec{p}_3 = 4|\vec{p}_1||\vec{p}_3| \cos \theta \quad (4.59)$$

in the rest frame of $\pi^+(p_2)$ and $\pi^-(p_3)$ with the expressions of $|\vec{p}_i|$ ($i = 1, 2, 3$) given in Eq. (4.14). Then we can write

$$\mathcal{A}_{\rho(770)} = -g^{\rho \rightarrow \pi^+\pi^-} F(s_{23}, m_\rho) T_\rho^{\text{GS}}(s_{23}) 2q \cos \theta \tilde{A}(B^- \rightarrow \rho\pi^-) + (s_{23} \leftrightarrow s_{12}), \quad (4.60)$$

with q already introduced in Eq. (4.14), where

$$\begin{aligned} \tilde{A}(B^- \rightarrow \rho\pi^-) = & \frac{G_F}{2} \sum_{p=u,c} \lambda_p^{(d)} \left\{ [\delta_{pu}(a_1 + \beta_2) + a_4^p + \dots]_{\rho\pi} \tilde{X}^{(B^-\rho,\pi)} \right. \\ & \left. + [\delta_{pu}(a_2 - \beta_2) - a_4^p + \dots]_{\pi\rho} \tilde{X}^{(B^-\pi,\rho)} \right\}, \end{aligned} \quad (4.61)$$

with

$$\begin{aligned} \tilde{X}^{(B^-\pi,\rho)} &= 2f_\rho m_B \tilde{p}_c F_1^{B\pi}(s_{23}), \\ \tilde{X}^{(B^-\rho,\pi)} &= 2f_\pi m_B \tilde{p}_c \left[A_0^{B\rho}(m_\pi^2) + \frac{1}{2m_\rho} \left(m_B - m_\rho - \frac{m_B^2 - s_{23}}{m_B + m_\rho} \right) A_2^{B\rho}(m_\pi^2) \right]. \end{aligned} \quad (4.62)$$

The decay rate is given by

$$\begin{aligned} \Gamma(B^- \rightarrow \rho\pi^- \rightarrow \pi^+\pi^-\pi^-) &= \frac{1}{2} \frac{1}{(2\pi)^3 32m_B^3} \int ds_{23} ds_{12} \left\{ \frac{|g^{\rho \rightarrow \pi^+\pi^-}|^2 F(s_{23}, m_\rho)^2 (1 + D\Gamma_\rho^0/m_\rho)^2}{(s_{23} - m_{f_2}^2 - f(s_{23}))^2 + m_\rho^2 \Gamma_\rho^2(s_{23})} \right. \\ & \left. \times 4q^2 \cos^2 \theta |\tilde{A}(B^- \rightarrow \rho\pi^-)|^2 + (s_{23} \leftrightarrow s_{12}) + \text{interference} \right\}. \end{aligned} \quad (4.63)$$

TABLE II: Numerical values of the flavor operators $a_i^p(M_1 M_2)$ for $M_1 M_2 = \rho(770)\pi$ and $\pi\rho(770)$ at the scale $\mu = \bar{m}_b(\bar{m}_b) = 4.18$ GeV.

a_i^p	$\rho\pi$	$\pi\rho$	a_i^p	$\rho\pi$	$\pi\rho$
a_1	$1.007 + 0.108i$	$1.000 + 0.095i$	a_6^c	$-0.045 - 0.005i$	$-0.013 - 0.006i$
a_2	$0.135 - 0.379i$	$0.158 - 0.340i$	a_7	$(-0.13 + 2.9i)10^{-4}$	$(-0.3 + 2.6i)10^{-4}$
a_3	$0.0008 + 0.0183i$	$-0.0004 + 0.016i$	a_8^u	$(5.2 - 1.0i)10^{-4}$	$(-8.9 - 8.5i)10^{-5}$
a_4^u	$-0.026 - 0.022i$	$-0.026 - 0.021i$	a_8^c	$(5.0 - 0.5i)10^{-4}$	$(-10.7 - 3.7i)10^{-5}$
a_4^c	$-0.030 - 0.013i$	$-0.031 - 0.012i$	a_9	$(-9.1 - 0.9i)10^{-3}$	$(-9.0 - 0.8i)10^{-3}$
a_5	$0.0018 - 0.0247i$	$0.004 - 0.022i$	a_{10}^u	$(-0.9 + 3.3i)10^{-3}$	$(-1.1 + 2.9i)10^{-3}$
a_6^u	$-0.042 - 0.014i$	$-0.010 - 0.015i$	a_{10}^c	$(-0.9 + 3.3i)10^{-3}$	$(-1.2 + 3.0i)10^{-3}$

One can integrate out the angular distribution part by noting that

$$\int_{(s_{12})_{\min}}^{(s_{12})_{\max}} ds_{12} \cos^2 \theta = \frac{2}{3a} = \frac{4}{3} \frac{m_B}{\sqrt{s_{23}}} q\tilde{p}_c. \quad (4.64)$$

In the narrow width limit,

$$\frac{m_\rho \Gamma_\rho(s)(1 + D \Gamma_\rho^0/m_\rho)^2}{(s - m_\rho^2 - f(s))^2 + m_\rho^2 \Gamma_\rho^2(s)} \xrightarrow{\Gamma_\rho \rightarrow 0} \pi \delta(s - m_\rho^2 - f(s)). \quad (4.65)$$

We see from Eq. (2.27) that $f(s)$ vanishes when $s \rightarrow m_\rho^2$. Hence, the δ -function implies $s \rightarrow m_\rho^2$ in the zero width limit. As a result, $\tilde{p}_c \rightarrow p_c$, $q \rightarrow q_0$, and $\tilde{A}(B^- \rightarrow \rho\pi^-) \rightarrow A(B^- \rightarrow \rho\pi^-)$. We then obtain the desired factorization relation

$$\Gamma(B^- \rightarrow \rho\pi^- \rightarrow \pi^+\pi^-\pi^-) \xrightarrow{\Gamma_\rho \rightarrow 0} \Gamma(B^- \rightarrow \rho\pi^-) \mathcal{B}(\rho \rightarrow \pi^+\pi^-), \quad (4.66)$$

where use of the relations

$$\Gamma_{\rho \rightarrow \pi^+\pi^-} = \frac{q_0^3}{6\pi m_\rho^2} g_{\rho \rightarrow \pi^+\pi^-}^2, \quad \Gamma_{B^- \rightarrow \rho\pi^-} = \frac{p_c}{8\pi m_B^2} |A(B^- \rightarrow \rho\pi^-)|^2, \quad (4.67)$$

has been made.

Numerical results

To compute the flavor operators $a_i^p(\rho\pi)$ and $a_i^p(\pi\rho)$ in QCDF, we need to specify the parameters $\rho_{A,H}$ and $\phi_{A,H}$ for penguin annihilation and hard spectator scattering diagrams. For $B \rightarrow VP$ decays, we use the superscripts ‘ i ’ and ‘ f ’

$$X_A^{i,f} = \ln \left(\frac{m_B}{\Lambda_h} \right) (1 + \rho_A^{i,f} e^{i\phi_A^{i,f}}), \quad (4.68)$$

to distinguish the gluon emission from the initial and final-state quarks, respectively. We shall use

$$(\rho_A^i, \rho_A^f)_{PV} = (2.87_{-1.95}^{+0.66}, 0.91_{-0.13}^{+0.12}), \quad (\phi_A^i, \phi_A^f)_{PV} = (-145_{-21}^{+14}, -37_{-9}^{+10})^\circ, \quad (4.69)$$

and the first order approximation of $\rho_H \approx \rho_A^i$ and $\phi_H \approx \phi_A^i$ (see [28] for details). This leads to

$$\begin{aligned}\beta_2^p(\rho\pi) &= 0.025 + 0.011i, & (\beta_3^p + \beta_{3,\text{EW}}^p)(\rho\pi) &= 0.034 - 0.030i, \\ \beta_2^p(\pi\rho) &= -0.018 - 0.008i, & (\beta_3^p + \beta_{3,\text{EW}}^p)(\pi\rho) &= 0.026 - 0.021i,\end{aligned}\quad (4.70)$$

and the flavor operators $a_i^p(\rho\pi)$ and $a_i^p(\pi\rho)$ shown in Table II.

Following [29], we obtain in QCDF

$$\begin{aligned}\mathcal{B}(B^- \rightarrow \rho(770)\pi^-)_{\text{QCDF}} &= (8.18_{-0.81}^{+1.67}) \times 10^{-6}, \\ \mathcal{A}_{CP}(B^- \rightarrow \rho(770)\pi^-)_{\text{QCDF}} &= (0.36_{-4.54}^{+5.36})\%,\end{aligned}\quad (4.71)$$

where use of the decay constants $f_\rho = 216$ MeV and $f_\rho^\perp(\mu = 1 \text{ GeV}) = 165$ MeV [29] has been made. For the finite-width $\Gamma_\rho^0 = 149.1 \pm 0.8$ MeV, we find

$$\begin{aligned}\mathcal{B}(B^- \rightarrow \rho(770)\pi^- \rightarrow \pi^+\pi^-\pi^-) &= (8.76_{-1.68}^{+1.86}) \times 10^{-6}, \\ \mathcal{A}_{CP}(B^- \rightarrow \rho(770)\pi^- \rightarrow \pi^+\pi^-\pi^-) &= -(0.24_{-0.54}^{+0.46})\%,\end{aligned}\quad (4.72)$$

and

$$\eta_{\rho\pi}^{\text{GS,QCDF}} = 0.931 \quad (0.855), \quad (4.73)$$

with negligible uncertainties, where the value in parentheses is obtained with $F(s, m_{f_2}) = 1$. The same results for $\eta_{\rho\pi}^{\text{GS,QCDF}}$ can also be obtained using Eqs. (2.31) and (4.60). The deviation of η_ρ^{GS} from unity at 7% level is contrasted with the ratio $\Gamma_\rho/m_\rho = 0.192$. For comparison, using the Breit-Wigner model to describe the ρ line shape, we get

$$\eta_{\rho\pi}^{\text{BW,QCDF}} = 1.111 \pm 0.001, \quad (1.033). \quad (4.74)$$

In the experimental parameterization scheme, we obtain

$$\eta_{\rho\pi}^{\text{GS,EXPP}} = 0.950, \quad \eta_{\rho\pi}^{\text{BW,EXPP}} = 1.152 \pm 0.001. \quad (4.75)$$

The parameter η_ρ as a function of the $\rho(770)$ width is shown in Fig. 3 for both Gounaris-Sakurai and Breit-Wigner line shape models and for both QCDF and EXPP schemes.

As shown in Eq. (2.32), the expression of η_ρ^{GS} is the same as that of η_ρ^{BW} except for an additional $r^2 \equiv (1 + D\Gamma_\rho^0/m_\rho)^2$ factor in the denominator. This r^2 term accounts for the fact that $\eta_\rho^{\text{GS}} < 1 < \eta_\rho^{\text{BW}}$ in both QCDF and EXPP schemes. Since the Gounaris-Sakurai line shape was employed by both BaBar and LHCb Collaborations in their analyses of the ρ resonance in $B^- \rightarrow \pi^+\pi^-\pi^-$ decay, the branching fraction of $B^- \rightarrow \rho\pi^-$ should be corrected using η_ρ^{GS} rather than η_ρ^{BW} .

From the measured branching fraction $\mathcal{B}(B^- \rightarrow \rho(770)\pi^- \rightarrow \pi^+\pi^-\pi^-) = (8.44 \pm 0.87) \times 10^{-6}$ by LHCb [9, 10] and $(8.1 \pm 0.7 \pm 1.2_{-1.1}^{+0.4}) \times 10^{-6}$ by BaBar [8], we obtain the world average

$$\mathcal{B}(B^- \rightarrow \rho(770)\pi^- \rightarrow \pi^+\pi^-\pi^-)_{\text{expt}} = (8.36 \pm 0.77) \times 10^{-6}. \quad (4.76)$$

It is worth emphasizing that the CP asymmetry for the quasi-two-body decay $B^- \rightarrow \rho^0\pi^-$ has been found by LHCb to be consistent with zero in all three S -wave approaches. For example, $\mathcal{A}_{CP}(\rho^0\pi^-) = (0.7 \pm 1.9)\%$ in the isobar model [9, 10]. However, previous theoretical predictions all lead to a negative CP asymmetry for $B^- \rightarrow \rho^0\pi^-$, ranging from -7% to -45% (see [28] for a detailed discussion). The QCDF results for the branching fraction and CP asymmetry presented in Eq. (4.72) agree with experiment.

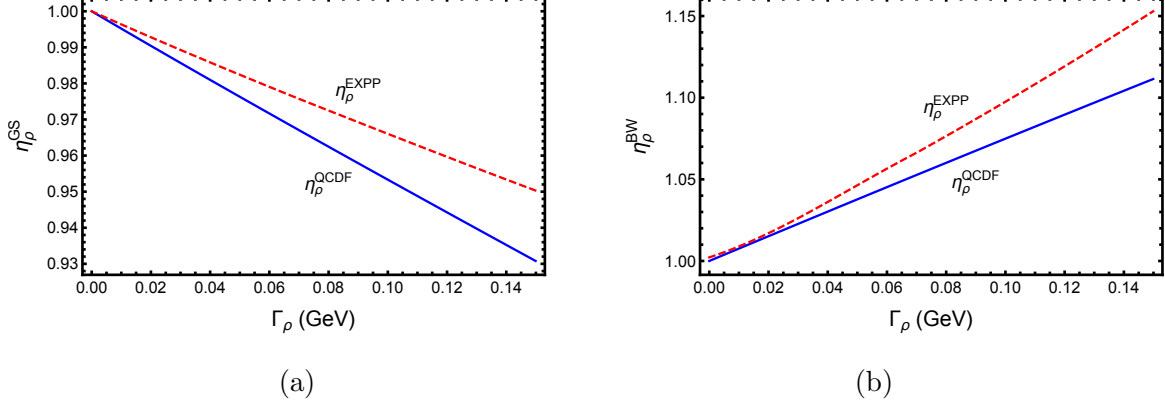


FIG. 3: Same as Fig. 1 for the $\rho(770)$ resonance mediating the $B^- \rightarrow \pi^+\pi^-\pi^-$ decay using (a) the Gounaris-Sakurai model and (b) the Breit-Wigner model to describe its line shape.

2. $\rho(770)K^-$

The three-body decay amplitude $\mathcal{A}_{\rho(770)K^-} \equiv A(B^- \rightarrow K^- \rho(770) \rightarrow K^-(p_1)\pi^+(p_2)\pi^-(p_3))$ has the expression

$$\begin{aligned}
\mathcal{A}_{\rho(770)K^-} &= -\frac{G_F}{2} \sum_{p=u,c} \lambda_p^{(s)} g^{\rho \rightarrow \pi^+\pi^-} F(s_{23}, m_\rho) T_\rho^{\text{GS}}(s_{23})(s_{12} - s_{13}) \\
&\quad \times \left\{ f_K \left[m_\rho A_0^{B\rho}(m_K^2) + \frac{1}{2} \left(m_B - m_\rho - \frac{m_B^2 - s_{23}}{m_B + m_\rho} \right) A_2^{B\rho}(m_K^2) \right] \right. \\
&\quad \quad \times \left[\delta_{pu}(a_1 + \beta_2) + a_4^p + a_{10}^p - r_\chi^K (a_6^p + a_8^p) + \beta_3^p + \beta_{3,\text{EW}}^p \right]_{\rho K} \\
&\quad \quad \left. + m_\rho f_\rho F_1^{BK}(s_{23}) \left[\delta_{pu} a_2 + \frac{3}{2}(a_7^p + a_9^p) \right]_{K\rho} \right\}, \\
&= -g^{\rho \rightarrow \pi^+\pi^-} F(s_{23}, m_\rho) T_\rho^{\text{GS}}(s_{23}) 2q \cos \theta \tilde{A}(B^- \rightarrow \rho K^-), \tag{4.77}
\end{aligned}$$

where use of Eq. (4.59) has been made, and $\tilde{A}(B^- \rightarrow \rho K^-)$ has the same expression as the QCDF amplitude for the quasi-two-body decay $B^- \rightarrow \rho K^-$ [14]

$$\begin{aligned}
A(B^- \rightarrow \rho K^-) &= \frac{G_F}{2} \sum_{p=u,c} \lambda_p^{(s)} \left\{ 2f_\rho m_B p_c F_1^{BK}(m_\rho^2) \left[\delta_{pu} a_2 + \frac{3}{2}(a_7^p + a_9^p) \right]_{K\rho} \right. \\
&\quad \left. + 2f_K m_B p_c A_0^{B\rho}(m_K^2) \left[\delta_{pu}(a_1 + \beta_2) + a_4^p + a_{10}^p - r_\chi^K (a_6^p + a_8^p) + \beta_3^p + \beta_{3,\text{EW}}^p \right]_{\rho K} \right\}, \tag{4.78}
\end{aligned}$$

except for a replacement of $p_c F_1^{BK}(m_\rho^2)$ by $\tilde{p}_c F_1^{BK}(s_{23})$ and $A_0^{B\rho}(m_K^2)$ by

$$A_0^{B\rho}(m_K^2) + \frac{1}{2m_\rho} \left(m_B - m_\rho - \frac{m_B^2 - s_{23}}{m_B + m_\rho} \right) A_2^{B\rho}(m_K^2). \tag{4.79}$$

In QCDF, we obtain

$$\begin{aligned}
\mathcal{B}(B^- \rightarrow \rho(770)K^-)_{\text{QCDF}} &= (4.03_{-1.67}^{+3.56}) \times 10^{-6}, \\
A_{CP}(B^- \rightarrow \rho(770)K^-)_{\text{QCDF}} &= (21.6_{-16.6}^{+17.1})\%. \tag{4.80}
\end{aligned}$$

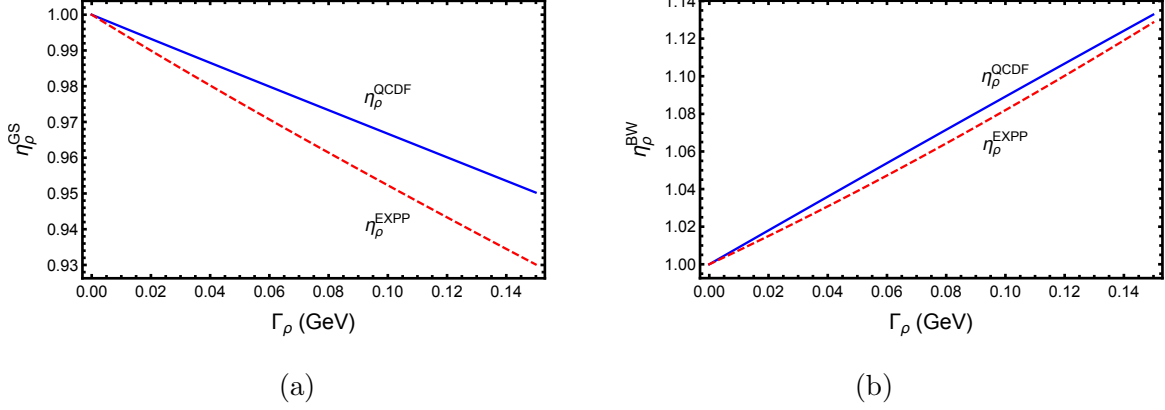


FIG. 4: Same as Fig. 3 except that the $\rho(770)$ state is the resonance produced in the decay $B^- \rightarrow K^- \pi^+ \pi^-$.

For the finite ρ width, we find

$$\begin{aligned} \mathcal{B}(B^- \rightarrow K^- \rho(770) \rightarrow K^- \pi^+ \pi^-) &= (4.23_{-0.84}^{+0.95}) \times 10^{-6}, \\ A_{CP}(B^- \rightarrow K^- \rho(770) \rightarrow K^- \pi^+ \pi^-) &= (20.5 \pm 0.8)\%, \end{aligned} \quad (4.81)$$

and

$$\eta_{\rho K}^{\text{GS,QCDF}} = 0.951 \pm 0.003, \quad (0.899). \quad (4.82)$$

As a comparison, if the Breit-Wigner model is used to describe the ρ line shape, we are led to have

$$\eta_{\rho K}^{\text{BW,QCDF}} = 1.132 \pm 0.001, \quad (1.086). \quad (4.83)$$

In the experimental parameterization scheme, we obtain

$$\eta_{\rho K}^{\text{GS,EXPP}} = 0.931, \quad \eta_{\rho K}^{\text{BW,EXPP}} = 1.128 \pm 0.001. \quad (4.84)$$

The dependence of η_ρ as a function of the $\rho(770)$ width is shown in Fig. 4 for both the Gounaris-Sakurai and Breit-Wigner line shape models. It is evident that $\eta_{\rho\pi}$ and $\eta_{\rho K}$ are close to each other, as it should be. Our predictions in Eq. (4.81) are consistent with the data:

$$\begin{aligned} \mathcal{B}(B^- \rightarrow K^- \rho(770) \rightarrow K^- \pi^+ \pi^-)_{\text{PDG}} &= (3.7 \pm 0.5) \times 10^{-6}, \\ A_{CP}(B^- \rightarrow K^- \rho(770) \rightarrow K^- \pi^+ \pi^-)_{\text{PDG}} &= 0.37 \pm 0.10. \end{aligned} \quad (4.85)$$

3. $K^*(892)$

For the three-body decay amplitude $\mathcal{A}_{K^*(892)} \equiv A(B^- \rightarrow \bar{K}^{*0}(892)\pi^- \rightarrow K^-(p_1)\pi^+(p_2)\pi^-(p_3))$, factorization leads to the expression

$$\begin{aligned} \mathcal{A}_{K^*(892)} &= -\frac{G_F}{\sqrt{2}} \sum_{p=u,c} \lambda_p^{(s)} g^{K^* \rightarrow K^- \pi^+} F(s_{12}, m_{K^*}) T_{K^*}^{\text{BW}}(s_{12}) \left[s_{13} - s_{23} - \frac{(m_B^2 - m_\pi^2)(m_K^2 - m_\pi^2)}{s_{12}} \right] \\ &\quad \times \left[a_4^p - \frac{1}{2} a_{10}^p + r_\chi^{K^*} (a_6^p - \frac{1}{2} a_8^p) + \delta_{pu} \beta_2^p + \beta_3^p + \beta_{3,\text{EW}}^p \right]_{\pi K^*} m_{K^*} f_{K^*} F_1^{B\pi}(s_{12}). \end{aligned} \quad (4.86)$$

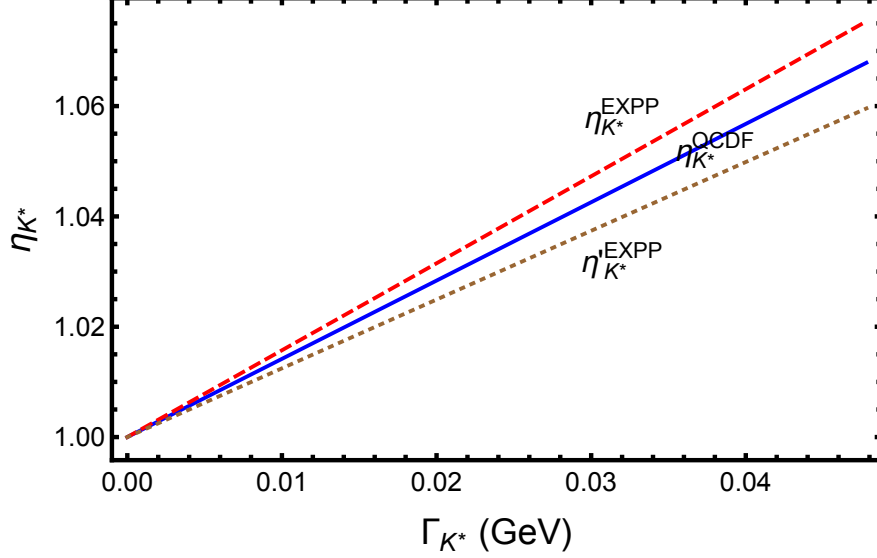


FIG. 5: Same as Fig. 1 for the resonance $K^*(892)$ produced in the three-body decay $B^- \rightarrow K^- \pi^+ \pi^-$.

Since

$$s_{13} - s_{23} - \frac{(m_B^2 - m_\pi^2)(m_{K^*}^2 - m_\pi^2)}{s_{12}} = 4\vec{p}_2 \cdot \vec{p}_3 = 4|\vec{p}_2||\vec{p}_3| \cos \theta \quad (4.87)$$

in the rest frame of $K^-(p_1)$ and $\pi^+(p_2)$, the three-body amplitude can be recast to

$$\mathcal{A}_{K^*(892)} = -g^{\bar{K}^* \rightarrow K^- \pi^+} F(s_{12}, m_{K^*}) T_{K^*}^{\text{BW}}(s_{12}) 2q \cos \theta \tilde{A}(B^- \rightarrow \bar{K}^{*0}(892)\pi^-), \quad (4.88)$$

where $\tilde{A}(B^- \rightarrow \bar{K}^{*0}(892)\pi^-)$ has the same expression as the QCDF amplitude for the quasi-two-body decay $B^- \rightarrow \bar{K}^{*0}(892)\pi^-$ [14]

$$A(B^- \rightarrow \bar{K}^{*0}\pi^-) = \frac{G_F}{\sqrt{2}} \sum_{p=u,c} \lambda_p^{(s)} \left[a_4^p - \frac{1}{2}a_{10}^p + r_\chi^{K^*} (a_6^p - \frac{1}{2}a_8^p) + \beta_2^p \delta_{pu} + \beta_3^p + \beta_{3,\text{EW}}^p \right]_{\pi K^*} 2f_{K^*} m_B p_c F_1^{B\pi}(m_{K^*}^2), \quad (4.89)$$

except for a replacement of $p_c F_1^{B\pi}(m_{K^*}^2)$ by $\tilde{p}_c F_1^{B\pi}(s_{12})$. It is then straightforward to show the factorization relation

$$\Gamma(B^- \rightarrow \bar{K}^{*0}(892)\pi^- \rightarrow K^- \pi^+ \pi^-) \xrightarrow{\Gamma_{K^*} \rightarrow 0} \Gamma(B^- \rightarrow \bar{K}^{*0}(892)\pi^-) \mathcal{B}(\bar{K}^{*0}(892) \rightarrow \pi^+ \pi^-) \quad (4.90)$$

being valid in the narrow width limit.

In QCDF, we obtain

$$\begin{aligned} \mathcal{B}(B^- \rightarrow \bar{K}^{*0}(892)\pi^-) &= (10.4_{-1.7}^{+1.8}) \times 10^{-6}, \\ A_{CP}(B^- \rightarrow \bar{K}^{*0}(892)\pi^-) &= (0.16_{-0.14}^{+0.17})\%, \end{aligned} \quad (4.91)$$

and

$$\beta_2^p(\pi K^*) = 0.017 + 0.006i, \quad (\beta_3^p + \beta_{3,\text{EW}}^p)(\pi K^*) = -0.027 + 0.022i. \quad (4.92)$$

For the finite-width $\Gamma_{K^*0}^0 = 47.3 \pm 0.5$ MeV, we find

$$\begin{aligned} \mathcal{B}(B^- \rightarrow \overline{K}^{*0}(892)\pi^- \rightarrow K^- \pi^+ \pi^-) &= (6.52_{-1.42}^{+1.59}) \times 10^{-6}, \\ A_{CP}(B^- \rightarrow \overline{K}^{*0}(892)\pi^- \rightarrow K^- \pi^+ \pi^-) &= (0.166 \pm 0.002)\%, \end{aligned} \quad (4.93)$$

and

$$\eta_{K^*}^{\text{BW,QCDF}} = 1.067 \pm 0.002, \quad (0.9914 \pm 0.0001). \quad (4.94)$$

As for the η_{K^*} parameter in the experimental parameterization, we obtain

$$\eta_{K^*}^{\text{EXPP}} = 1.075 \pm 0.001, \quad \eta'_{K^*}{}^{\text{EXPP}} = 1.059 \pm 0.001. \quad (4.95)$$

The dependence of η_{K^*} in QCDF and in experimental parameterization is shown in Fig. 5.

The deviation of η_{K^*} from unity is roughly consistent with the expectation from the ratio $\Gamma_{K^*}/m_{K^*} = 0.053$. Experimentally, the average of BaBar [12] and Belle [30] measurements yields

$$\mathcal{B}(B^- \rightarrow \overline{K}^{*0}(892)\pi^- \rightarrow K^- \pi^+ \pi^-)_{\text{expt}} = (6.71 \pm 0.57) \times 10^{-6}. \quad (4.96)$$

The result of the QCDF calculation of the branching fraction given in Eq. (4.93) agrees with experimental data.

C. Scalar resonances

For examples of scalar intermediate states, we shall take the processes $B^- \rightarrow \sigma/f_0(500)\pi^- \rightarrow \pi^+\pi^-\pi^-$ and $B^- \rightarrow \overline{K}_0^*(1430)\pi^- \rightarrow K^-\pi^+\pi^-$ to illustrate their finite-width effects. Since $K_0^*(1430)$ and especially σ are very broad, they are expected to exhibit large width effects.¹⁰

1. $\sigma/f_0(500)$

In QCDF, the decay amplitude of $B^- \rightarrow \sigma\pi^-$ is given by (see Eq. (A6) of [32]):

$$\begin{aligned} A(B^- \rightarrow \sigma\pi^-) &= \frac{G_F}{\sqrt{2}} \sum_{p=u,c} \lambda_p^{(d)} \left\{ [a_1 \delta_{pu} + a_4^p + a_{10}^p - (a_6^p + a_8^p) r_\chi^\pi]_{\sigma\pi} X^{(B\sigma,\pi)} \right. \\ &\quad + \left[a_2 \delta_{pu} + 2(a_3^p + a_5^p) + \frac{1}{2}(a_7^p + a_9^p) + a_4^p - \frac{1}{2}a_{10}^p - (a_6^p - \frac{1}{2}a_8^p) r_\chi^\sigma \right]_{\pi\sigma} X^{(B\pi,\sigma)} \\ &\quad \left. - f_B f_\pi \bar{f}_\sigma^u \left[\delta_{pu} b_2(\pi\sigma) + b_3(\pi\sigma) + b_{3,\text{EW}}(\pi\sigma) + (\pi\sigma \rightarrow \sigma\pi) \right] \right\}, \end{aligned} \quad (4.97)$$

where the factorizable matrix elements read

$$X^{(B\sigma,\pi)} = -f_\pi F_0^{B\sigma u}(m_\pi^2)(m_B^2 - m_\sigma^2), \quad X^{(B\pi,\sigma)} = \bar{f}_\sigma^u F_0^{B\pi}(m_\sigma^2)(m_B^2 - m_\pi^2), \quad (4.98)$$

¹⁰ The finite-width effect for $\sigma/f_0(500)$ had been considered in [31].

and $\bar{r}_\chi^\sigma(\mu) = 2m_\sigma/m_b(\mu)$. The superscript u in the scalar decay constant \bar{f}_σ^u and the form factor $F^{B\sigma^u}$ refers to the u quark component of the σ meson. The scale-dependent scalar decay constant is defined by $\langle\sigma|\bar{u}u|0\rangle = m_\sigma\bar{f}_\sigma^u$. We follow [28] to take $\bar{f}_\sigma^u = 350$ MeV at $\mu = 1$ GeV and $F_0^{B\sigma^u}(0) = 0.25$, where the Clebsch-Gordon coefficient $1/\sqrt{2}$ is included in \bar{f}_σ^u and $F_0^{B\sigma^u}$.

As discussed in Sec. II.E, the σ is too broad to be described by the usual Breit-Wigner line shape.¹¹ We thus follow the LHCb Collaboration [10] to use the simple pole description¹²

$$T_\sigma(s) = \frac{1}{s - s_\sigma} = \frac{1}{s - m_\sigma^2 + \Gamma_\sigma^2(s)/4 + im_\sigma\Gamma_\sigma(s)}, \quad (4.99)$$

with $\sqrt{s_\sigma} = m_\sigma - i\Gamma_\sigma/2$ and

$$\Gamma_\sigma(s) = \Gamma_\sigma^0 \left(\frac{q}{q_0} \right) \frac{m_\sigma}{\sqrt{s}}. \quad (4.100)$$

Using the isobar description of the $\pi^+\pi^-$ S -wave to fit the $B^+ \rightarrow \pi^+\pi^-\pi^+$ decay data, the LHCb Collaboration found [10]

$$\sqrt{s_\sigma} = (563 \pm 10) - i(350 \pm 13) \text{ MeV}, \quad (4.101)$$

consistent with the PDG value of $\sqrt{s_\sigma} = (400 - 550) - i(200 - 350) \text{ MeV}$ [3].

With $\mathcal{A}_\sigma \equiv A(B^- \rightarrow \sigma\pi^- \rightarrow \pi^+\pi^-\pi^-)$, factorization leads to [17]

$$\begin{aligned} \mathcal{A}_\sigma &= \frac{G_F}{2} \sum_{p=u,c} \lambda_p^{(d)} g^{\sigma \rightarrow \pi^+\pi^-} F(s_{23}, m_\sigma) T_\sigma(s_{23}) \left\{ \tilde{X}^{(B\sigma,\pi)} [a_1\delta_{pu} + a_4^p + a_{10}^p - (a_6^p + a_8^p)r_\chi^\pi]_{\sigma\pi} \right. \\ &\quad \left. + \tilde{X}^{(B\pi,\sigma)} \left[a_2\delta_{pu} + 2(a_3^p + a_5^p) + \frac{1}{2}(a_7^p + a_9^p) + a_4^p - \frac{1}{2}a_{10}^p - (a_6^p - \frac{1}{2}a_8^p)\bar{r}_\chi^\sigma \right]_{\pi\sigma} \right\} \\ &\quad + (s_{23} \leftrightarrow s_{12}) \\ &= g^{\sigma \rightarrow \pi^+\pi^-} F(s_{23}, m_\sigma) T_\sigma(s_{23}) \tilde{A}(B^- \rightarrow \sigma\pi^-) + (s_{23} \leftrightarrow s_{12}), \end{aligned} \quad (4.102)$$

with

$$\tilde{X}^{(B\sigma,\pi)} = -f_\pi(m_B^2 - s_{23})F_0^{B\sigma^u}(m_\pi^2), \quad \tilde{X}^{(B\pi,\sigma)} = \bar{f}_\sigma^u(m_B^2 - m_\pi^2)F_0^{B\pi}(s_{23}). \quad (4.103)$$

Its decay rate reads

$$\begin{aligned} \Gamma(B^- \rightarrow \sigma\pi^- \rightarrow \pi^+\pi^-\pi^-) &= \frac{1}{2} \frac{1}{(2\pi)^3 32m_B^3} \int ds_{23} ds_{12} \left\{ \frac{|g^{\sigma \rightarrow \pi^+\pi^-}|^2 F(s_{23}, m_\sigma)^2}{(s_{23} - m_\sigma^2 + \Gamma_\sigma(s_{23})/4)^2 + m_\sigma^2 \Gamma_\sigma^2(s_{23})} \right. \\ &\quad \left. \times |\tilde{A}(B^- \rightarrow \sigma\pi^-)|^2 + (s_{23} \leftrightarrow s_{12}) + \text{interference} \right\}. \end{aligned} \quad (4.104)$$

¹¹ Another issue with the Breit-Wigner line shape is that the Breit-Wigner mass and width agree with the pole parameters only if the resonance is narrow.

¹² In the analysis of $B^0 \rightarrow \bar{D}^0\pi^+\pi^-$ decays [33], LHCb has adopted the Bugg model [34] to describe the line shape of $\sigma/f_0(500)$. However, the parameterization used in this model is rather complicated and the mass parameter $M \sim 1$ GeV is not directly related to the σ pole mass. Hence, we shall follow [10] to assume a simple pole model.

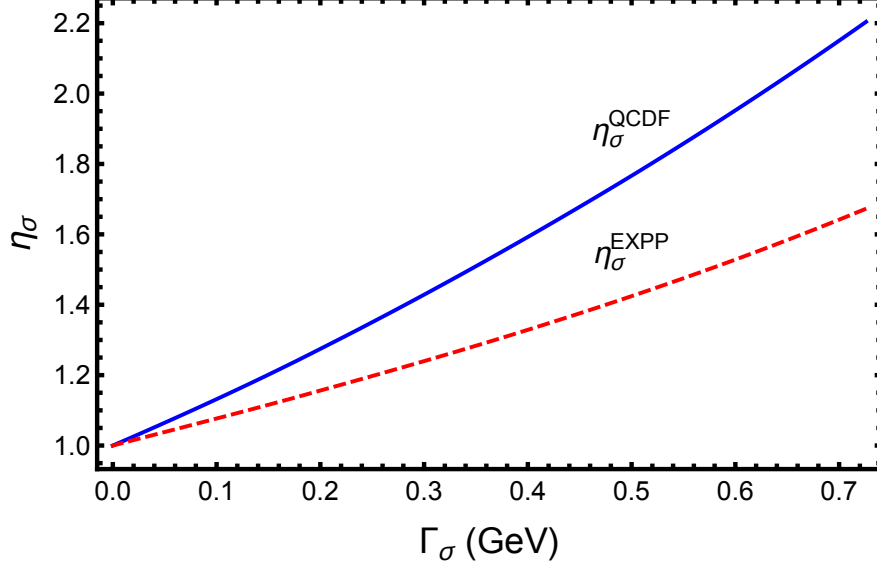


FIG. 6: The parameter η_σ as a function of the σ width, where the solid curve is derived from the QCDF calculation and the dashed curve from the experimental parameterization (EXPP).

Note that

$$\int_{(s_{12})_{\min}}^{(s_{12})_{\max}} ds_{12} = \frac{2}{a} = 4 \frac{m_B}{\sqrt{s_{23}}} q \tilde{p}_c. \quad (4.105)$$

Applying the relations

$$\Gamma_{\sigma \rightarrow \pi^+ \pi^-} = \frac{q_0}{8\pi m_\sigma^2} g_{\sigma \rightarrow \pi^+ \pi^-}^2, \quad \Gamma_{B^- \rightarrow \sigma \pi^-} = \frac{p_c}{8\pi m_B^2} |A(B^- \rightarrow \sigma \pi^-)|^2, \quad (4.106)$$

we arrive at the desired factorization relation¹³

$$\Gamma(B^- \rightarrow \sigma \pi^- \rightarrow \pi^+ \pi^- \pi^-) \xrightarrow{\Gamma_\sigma \rightarrow 0} \Gamma(B^- \rightarrow \sigma \pi^-) \mathcal{B}(\sigma \rightarrow \pi^+ \pi^-). \quad (4.107)$$

Using the input parameters given in [17], we obtain

$$\begin{aligned} \mathcal{B}(B^- \rightarrow \sigma \pi^-)_{\text{QCDF}} &= (5.31_{-0.19-1.18-1.33}^{+0.20+1.33+0.89}) \times 10^{-6}, \\ A_{CP}(B^- \rightarrow \sigma \pi^-)_{\text{QCDF}} &= (15.06_{-0.29-0.03-11.34}^{+0.30+0.02+8.34})\% \end{aligned} \quad (4.108)$$

in QCDF. For the finite-width $\Gamma_\sigma^0 = 700 \pm 26$ MeV, we find

$$\begin{aligned} \mathcal{B}(B^- \rightarrow \sigma \pi^- \rightarrow \pi^+ \pi^- \pi^-) &= (1.65_{-0.37}^{+0.42}) \times 10^{-6}, \\ A_{CP}(B^- \rightarrow \sigma \pi^- \rightarrow \pi^+ \pi^- \pi^-) &= (14.7 \pm 0.1)\%, \end{aligned} \quad (4.109)$$

¹³ In the LHCb paper, the square of the pole position is defined by $\sqrt{s_\sigma} = m_\sigma - i\Gamma_\sigma$ rather than $m_\sigma - i\Gamma_\sigma/2$. In this case, the left-hand side of the factorization relation in Eq. (4.107) should be multiplied by a factor of 2.

and

$$\begin{aligned}\eta_\sigma^{\text{QCDF}} &= 2.15 \pm 0.05 \quad (1.629 \pm 0.025), \\ \eta_\sigma^{\text{EXPP}} &= 1.64 \pm 0.03,\end{aligned}\tag{4.110}$$

where use of Eq. (2.37) has been made for the calculation of $\eta_\sigma^{\text{EXPP}}$. The dependence of η_σ on the σ width is shown in Fig. 6. Thus, the width correction is very large here. In Sec. V.B, we shall discuss its implications.

The LHCb measurement analyzed in the isobar model [9, 10] yields

$$\begin{aligned}\mathcal{B}(B^- \rightarrow \sigma\pi^- \rightarrow \pi^+\pi^-\pi^-)_{\text{expt}} &= (3.83 \pm 0.84) \times 10^{-6}, \\ A_{CP}(B^- \rightarrow \sigma\pi^- \rightarrow \pi^+\pi^-\pi^-)_{\text{expt}} &= (14.9_{-0.6}^{+0.5})\%.\end{aligned}\tag{4.111}$$

We see that while the calculated CP asymmetry in Eq. (4.109) based on QCDF is in excellent agreement with experiment, the predicted branching fraction is smaller than the measurement by a factor of about 2.

2. $K_0^*(1430)$

For the three-body decay amplitude $\mathcal{A}_{K_0^*(1430)} \equiv A(B^- \rightarrow \bar{K}_0^*(1430)^0\pi^- \rightarrow K^-(p_1)\pi^+(p_2)\pi^-(p_3))$, factorization leads to the expression

$$\begin{aligned}\mathcal{A}_{K_0^*(1430)} &= \frac{G_F}{\sqrt{2}} \sum_{p=u,c} \lambda_p^{(s)} g^{K_0^* \rightarrow K^- \pi^+} F(s_{12}, m_{K_0^*}) T_{K_0^*}^{\text{BW}}(s_{12}) \left[a_4^p - \frac{1}{2} a_{10}^p - r_\chi^{K_0^*} \left(\frac{s_{12}}{m_{K_0^*}^2} \right) \left(a_6^p - \frac{1}{2} a_8^p \right) \right. \\ &\quad \left. + \delta_{pu} \beta_2^p + \beta_3^p + \beta_{3,\text{EW}}^p \right]_{\pi K^*} f_{\bar{K}_0^*} F_0^{B\pi}(s_{12})(m_B^2 - m_\pi^2) \\ &= g^{K_0^* \rightarrow K^- \pi^+} F(s_{12}, m_{K_0^*}) T_{K_0^*}^{\text{BW}}(s_{12}) \tilde{A}(B^- \rightarrow \bar{K}_0^*(1430)^0\pi^-),\end{aligned}\tag{4.112}$$

where

$$r_\chi^{K_0^*}(\mu) = \frac{2m_{K_0^*}^2}{m_b(\mu)(m_s(\mu) - m_q(\mu))},\tag{4.113}$$

and the vector decay constant of $\bar{K}_0^*(1430)$ is related to the scalar one defined by $\langle \bar{K}_0^* | \bar{s}d | 0 \rangle = m_{K_0^*} \bar{f}_{\bar{K}_0^*}$ via ¹⁴

$$f_{\bar{K}_0^*} = \frac{m_s(\mu) - m_q(\mu)}{m_{K_0^*}} \bar{f}_{\bar{K}_0^*}.\tag{4.114}$$

In QCDF, the decay amplitude of $B^- \rightarrow \bar{K}_0^{*0}\pi^-$ reads [32]

$$\begin{aligned}A(B^- \rightarrow \bar{K}_0^{*0}\pi^-) &= \frac{G_F}{\sqrt{2}} \sum_{p=u,c} \lambda_p^{(s)} \left[a_4^p - r_\chi^{K_0^*} a_6^p - \frac{1}{2} (a_{10}^p - r_\chi^{K_0^*} a_8^p) + \delta_{pu} \beta_2^p + \beta_3^p + \beta_{3,\text{EW}}^p \right]_{\pi K_0^*} \\ &\quad \times f_{\bar{K}_0^*} F_0^{B\pi}(m_{K_0^*}^2)(m_B^2 - m_\pi^2).\end{aligned}\tag{4.115}$$

¹⁴ The decay constants of a scalar meson and its antiparticle are related by $\bar{f}_{\bar{s}} = \bar{f}_s$ and $f_{\bar{s}} = -f_s$ [35]. Hence, the vector decay constants of $K_0^*(1430)$ and $\bar{K}_0^*(1430)$ are of opposite signs. Using the QCD sum rule result for $\bar{f}_{\bar{K}_0^*}$ [32], we obtain $f_{\bar{K}_0^*(1430)} = 36.4$ MeV.

It is obvious that $\tilde{A}(B^- \rightarrow \bar{K}_0^*(1430)^0 \pi^-)$ has the same expression as $A(B^- \rightarrow \bar{K}_0^* \pi^-)$ except that the chiral factor $r_\chi^{K_0^*}$ is multiplied by a factor of $s_{12}/m_{K_0^*}^2$ (see also [36]) and the form factor $F_0^{B\pi}(m_{K_0^*}^2)$ is replaced by $F_0^{B\pi}(s_{12})$. As before, we have the factorization relation

$$\Gamma(B^- \rightarrow \bar{K}_0^* \pi^- \rightarrow K^- \pi^+ \pi^-) \xrightarrow{\Gamma_{K_0^* \rightarrow 0}} \Gamma(B^- \rightarrow \bar{K}_0^* \pi^-) \mathcal{B}(\bar{K}_0^* \rightarrow \pi^+ \pi^-). \quad (4.116)$$

Following [32, 35], we obtain

$$\beta_2^p(\pi K_0^*) = -0.0969, \quad (\beta_3^p + \beta_{3,\text{EW}}^p)(\pi K_0^*) = -0.0323, \quad (4.117)$$

and

$$\begin{aligned} \mathcal{B}(B^- \rightarrow \bar{K}_0^*(1430)^0 \pi^-) &= (13.6_{-9.3}^{+39.9}) \times 10^{-6}, \\ A_{CP}(B^- \rightarrow \bar{K}_0^*(1430)^0 \pi^-) &= (1.27_{-4.75}^{+5.84})\%. \end{aligned} \quad (4.118)$$

For the finite-width $\Gamma_{K_0^*(1430)} = 270 \pm 80$ MeV, we find

$$\begin{aligned} \mathcal{B}(B^- \rightarrow \bar{K}_0^*(1430)^0 \pi^- \rightarrow K^- \pi^+ \pi^-) &= (10.2_{-2.3}^{+3.0}) \times 10^{-6}, \\ A_{CP}(B^- \rightarrow \bar{K}_0^*(1430)^0 \pi^- \rightarrow K^- \pi^+ \pi^-) &= (1.12 \pm 0.01)\%, \end{aligned} \quad (4.119)$$

and

$$\begin{aligned} \eta_{K_0^*}^{\text{QCDF}} &= 0.83 \pm 0.04, \quad (0.31_{-0.05}^{+0.08}), \\ \eta_{K_0^*}^{\text{EXPP}} &= 1.11 \pm 0.03. \end{aligned} \quad (4.120)$$

The dependence of $\eta_{K_0^*}$ on the $K_0^*(1430)$ width in the Breit-Wigner model is shown in Fig. 7. When off-shell effects on the strong coupling $g^{\bar{K}_0^* \rightarrow K^- \pi^+}$ are turned off, $\eta_{K_0^*}^{\text{QCDF}}$ is of order 0.30, rendering an extremely large deviation from unity, even much larger than η_σ . Off-shell effects are particularly significant in this mode because the seemingly large QCDF enhancement in the large s_{12} region is suppressed by the form factor $F(s_{12}, m_{K_0^*}^2)$. As a consequence, $\eta_{K_0^*}^{\text{QCDF}}$ becomes about 0.83.

It has been argued that the Breit-Wigner parameterization is not appropriate for describing the broad $K_0^*(1430)$ resonance. LASS line shape is an alternative and popular description of the $K_0^*(1430)$ component proposed by the LASS Collaboration [37]. In the analysis of three-body decays of B mesons, BaBar and Belle often adopt different definitions for the $K_0^*(1430)$ resonance and nonresonant. While Belle (see, *e.g.*, [30]) employed the relativistic Breit-Wigner model to describe the line shape of the $K_0^*(1430)$ resonance and an exponential parameterization for the nonresonant contribution, BaBar [12] used the LASS parameterization to describe the elastic $K\pi$ S -wave and the $K_0^*(1430)$ resonance by a single amplitude [37]

$$T_{K_0^*}^{\text{LASS}}(s) = \frac{\sqrt{s}}{q \cot \delta_B - iq} - e^{2i\delta_B} \frac{m_0 \Gamma_0 \frac{m_0}{q_0}}{s - m_0^2 + im_0 \Gamma_0 \frac{q}{q_0} \frac{m_0}{\sqrt{s}}}, \quad (4.121)$$

with

$$\cot \delta_B = \frac{1}{aq} + \frac{1}{2}rq, \quad (4.122)$$

where q is the c.m. momentum of K^- and π^+ in the $K_0^*(1430)$ rest frame and q_0 is the value of q when $s = m_{K_0^*}^2$. The second term of $T_{K_0^*}^{\text{LASS}}$ is similar to the relativistic Breit-Wigner function

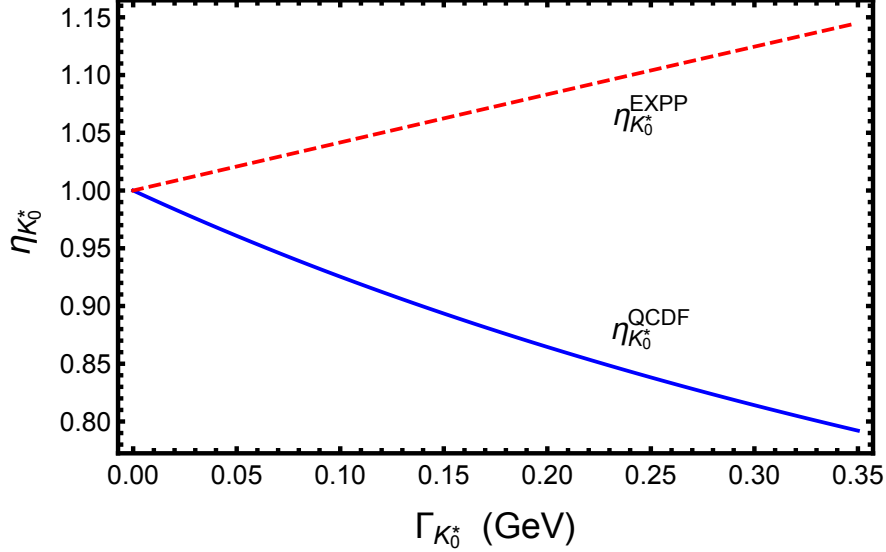


FIG. 7: Same as Fig. 6 for the resonance $\bar{K}_0^*(1430)$ produced in the three-body decay $B^- \rightarrow K^- \pi^+ \pi^-$.

TABLE III: Branching fractions (in units of 10^{-6}) of resonant and nonresonant (NR) contributions to $B^- \rightarrow K^- \pi^+ \pi^-$. Note that the BaBar's branching fraction $(2.4 \pm 0.5_{-1.5}^{+1.3}) \times 10^{-6}$ given in Table II of [12] is for the phase-space nonresonant contribution to $B^- \rightarrow K^- \pi^+ \pi^-$.

Decay mode	BaBar [12]	Belle [30]
$\bar{K}_0^{*0}(1430)\pi^-$	$19.8 \pm 0.7 \pm 1.7_{-0.9}^{+5.6} \pm 3.2$	$32.0 \pm 1.0 \pm 2.4_{-1.9}^{+1.1}$
NR	$9.3 \pm 1.0 \pm 1.2_{-0.4}^{+6.7} \pm 1.2$	$16.9 \pm 1.3 \pm 1.3_{-0.9}^{+1.1}$

$T_{K_0^*}^{\text{BW}}$ except for a phase factor δ_B introduced to retain unitarity. The first term is a slowly varying nonresonant component.

The nonresonant branching fraction $(2.4 \pm 0.5_{-1.5}^{+1.3}) \times 10^{-6}$ in $B^- \rightarrow K^- \pi^+ \pi^-$ reported by BaBar [12] is much smaller than $(16.9 \pm 1.3_{-1.6}^{+1.7}) \times 10^{-6}$ measured by Belle (see Table III). In the BaBar analysis, the nonresonant component of the Dalitz plot is modeled as a constant complex phase-space amplitude. Since the first part of the LASS line shape is really nonresonant, it should be added to the phase-space nonresonant piece to get the total nonresonant contribution. Indeed, by combining coherently the nonresonant part of the LASS parameterization and the phase-space nonresonant, BaBar found the total nonresonant branching fraction to be $(9.3 \pm 1.0 \pm 1.2_{-1.3}^{+6.8}) \times 10^{-6}$. Evidently, the BaBar result is now consistent with Belle within errors. For the resonant contributions from $K_0^*(1430)$, the BaBar results were obtained from $(K\pi)_0^* \pi^-$ by subtracting the elastic range term from the $K\pi$ S -wave [12], namely, the Breit-Wigner component of the LASS

parameterization.¹⁵ Although both BaBar and Belle employed the Breit-Wigner model to describe the line shape of $K_0^*(1430)$, the discrepancy between BaBar and Belle for the $K_0^*\pi$ mode remains an issue to be resolved.

Note that our calculation of $\mathcal{B}(B^- \rightarrow \overline{K}_0^*(1430)^0 \pi^- \rightarrow K^- \pi^+ \pi^-)$ in Eq. (4.119) based on QCDF is smaller by a factor of 2 (3) when compared to the BaBar (Belle) measurement. If we follow PDG [3] to apply the naïve factorization relation (1.1), we will obtain using Table III the branching fraction of $B^- \rightarrow \overline{K}_0^*(1430)\pi^-$ to be $(32.0 \pm 1.2_{-6.0}^{+10.8}) \times 10^{-6}$ from BaBar¹⁶ and $(51.6 \pm 1.7_{-7.5}^{+7.0}) \times 10^{-6}$ from Belle. Obviously, they are much larger than the QCDF prediction given in Eq. (4.118). Indeed, as pointed out before [32, 35], this has been a long-standing puzzle that for scalar resonances produced in B decays, the QCDF predictions of $B^- \rightarrow \overline{K}_0^*(1430)\pi^-$ and $\overline{B}^0 \rightarrow K_0^*(1430)\pi^+$ are in general too small compared to experiment by a factor of $2 \sim 4$. Nevertheless, when the finite-width effect is taken into account, the PDG values of $\mathcal{B}(B^- \rightarrow \overline{K}_0^*(1430)\pi^-)$ should be reduced by multiplying a factor of $\eta_{K_0^*}^{\text{QCDF}} \simeq 0.83$ or further enhanced by a factor of $\eta_{K_0^*}^{\text{EXPP}} \simeq 1.10$, depending on the scheme.

V. DISCUSSIONS

A. Finite-width and off-shell effects

In Table IV, we give a summary of the η_R parameters calculated using QCDF and the experimental parameterization for various resonances produced in the three-body B decays. Since the strong coupling of $R(m_{12}) \rightarrow P_1 P_2$ will be suppressed by the form factor $F(s_{12}, m_R)$ when m_{12} is off shell from m_R (see Eq. (4.20)), this implies a suppression of the three-body decay rate in the presence of off-shell effects. Therefore, η_R^{QCDF} is always larger than $\bar{\eta}_R^{\text{QCDF}}$, with the latter defined for $F(s, m_R) = 1$. We see from Table IV that off-shell effects are small in vector meson productions, but prominent in the $K_2^*(1430)$, $\sigma/f_0(500)$ and $K_0^*(1430)$ resonances. Also, the parameters η_R^{QCDF} and η_R^{EXPP} are similar for vector mesons, but different for tensor and scalar resonances. To understand the origin of their differences, we need to study the differential decay rates.

In Fig. 8, we show the normalized differential rates of the $B^- \rightarrow R\pi^- \rightarrow K^- \pi^+ \pi^-$ and $B^- \rightarrow K^- R \rightarrow K^- \pi^+ \pi^-$ decays with $R = \overline{K}^{*0}(980)$, $\overline{K}_0^{*0}(1430)$, $\overline{K}_2^0(1430)$ and ρ^0 respectively in the left plots. The plots blown up in the resonance regions are also shown in the right plots. Note that the figures on the right are scaled by a factor of $(\pi/2)\Gamma_R$ or $(\pi/2r^2)\Gamma_\rho^0$ with $r \equiv (1 + D\Gamma_\rho^0/m_\rho)$. For the $B^- \rightarrow K^- \rho^0 \rightarrow K^- \pi^+ \pi^-$ decay, we only show the result using the Gounaris-Sakurai line shape, as this is employed by the experimental parameterization for the ρ resonance. The normalized differential rates obtained from the QCDF calculation and the experimental parameterization are shown in the plots. For $R = \overline{K}^{*0}$ and \overline{K}_2^0 , we also show the results using the experimental

¹⁵ It should be stressed that the Breit-Wigner component of the LASS parameterization does not lead to the factorization relation Eq. (4.116).

¹⁶ Another BaBar measurement of $B^+ \rightarrow K_0^{*0}\pi^+ \rightarrow K_S^0\pi^0\pi^+$ [38] yields $\mathcal{B}(B^+ \rightarrow K_0^*(1430)\pi^+)_{\text{NWA}} = (34.6 \pm 3.3 \pm 4.6) \times 10^{-6}$.

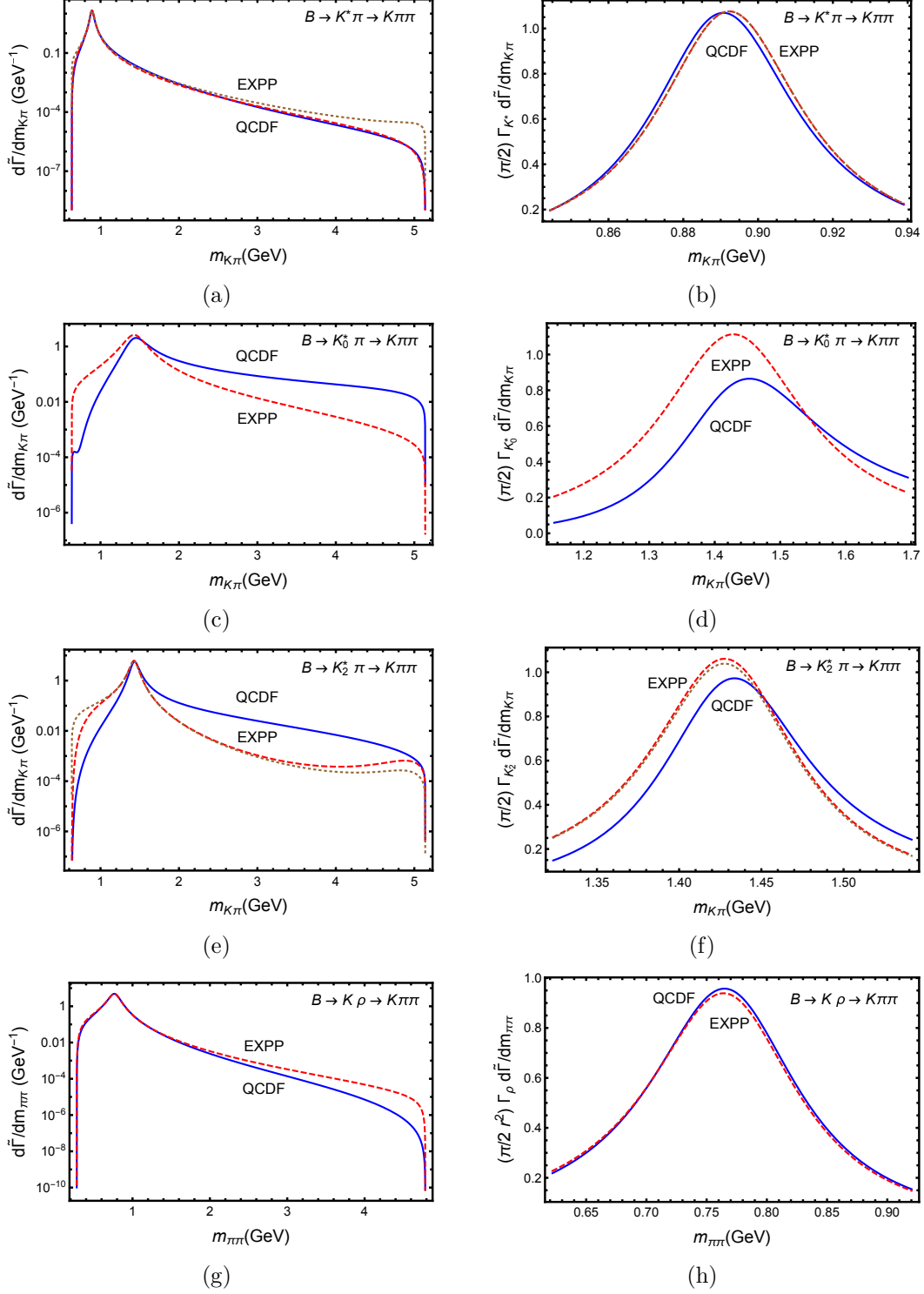


FIG. 8: Left column: the normalized differential rates in $B^- \rightarrow R\pi^- \rightarrow K^- \pi^+ \pi^-$ and $B^- \rightarrow K^- \rho \rightarrow K^- \pi^+ \pi^-$ decays. Right column: plots scaled and blown-up in the resonance regions, where the heights at the resonances equal η_R . In plot (h), we use $r \equiv 1 + D \Gamma_{\rho}^0 / m_{\rho}$. The solid curves come from the QCDF calculation and the dashed (dotted) curves from the experimental parameterization with (without) the transversality condition imposed.

TABLE IV: A summary of the η_R parameter for various resonances produced in the three-body B decays. Off-shell effects on the strong coupling $g^{R \rightarrow h_1 h_2}$ are taken into account in the determination of η_R^{QCDF} but not in $\bar{\eta}_R^{\text{QCDF}}$. Uncertainties in η_R are not specified whenever negligible.

Resonance	$B^+ \rightarrow R h_3 \rightarrow h_1 h_2 h_3$	Γ_R (MeV) [3]	Γ_R/m_R	$\bar{\eta}_R^{\text{QCDF}}$	η_R^{QCDF}	η_R^{EXPP}
$f_2(1270)$	$B^+ \rightarrow f_2 \pi^+ \rightarrow \pi^+ \pi^- \pi^+$	$186.7_{-2.5}^{+2.2}$	0.146	0.974	$1.003_{-0.002}^{+0.001}$	$0.937_{-0.005}^{+0.006}$
$K_2^*(1430)$	$B^+ \rightarrow K_2^{*0} \pi^+ \rightarrow K^+ \pi^- \pi^+$	109 ± 5	0.076	0.715 ± 0.009	0.972 ± 0.001	1.053 ± 0.002
$\rho(770)$	$B^+ \rightarrow \rho^0 \pi^+ \rightarrow \pi^+ \pi^- \pi^+$	149.1 ± 0.8	0.192	0.86 (GS) 1.03 (BW)	0.93 (GS) 1.11 (BW)	0.95 (GS) 1.15 (BW)
$\rho(770)$	$B^+ \rightarrow K^+ \rho^0 \rightarrow K^+ \pi^+ \pi^-$	149.1 ± 0.8	0.192	0.90 (GS) 1.09 (BW)	0.95 (GS) 1.13 (BW)	0.93 (GS) 1.13 (BW)
$K^*(892)$	$B^+ \rightarrow K^{*0} \pi^+ \rightarrow K^+ \pi^- \pi^+$	47.3 ± 0.5	0.053	1.01	1.067 ± 0.002	1.075
$\sigma/f_0(500)$	$B^+ \rightarrow \sigma \pi^+ \rightarrow \pi^+ \pi^- \pi^+$	700 ± 26 [10]	≈ 1.24	1.63 ± 0.03	2.15 ± 0.05	1.64 ± 0.03
$K_0^*(1430)$	$B^+ \rightarrow K_0^{*0} \pi^+ \rightarrow K^+ \pi^- \pi^+$	270 ± 80	≈ 0.19	$0.31_{-0.05}^{+0.08}$	0.83 ± 0.04	1.11 ± 0.03

parameterization with or without enforcing the transversality condition (see Eqs. (3.2) and (3.10)). They are plotted in dashed and dotted curves, respectively. Removing the transversality condition has mild effects on the normalized differential rates and little impacts on their values at the resonances.

As shown in Eqs. (2.20) and (2.32), η_R in these decays are given by

$$\eta_R = \frac{1}{2} \pi \Gamma_R \frac{d\tilde{\Gamma}(m_R)}{dm_{K\pi}}, \quad \eta_\rho^{\text{GS}} = \frac{\pi \Gamma_\rho^0}{2(1 + D \Gamma_\rho^0/m_\rho)^2} \frac{d\tilde{\Gamma}(m_\rho)}{dm_{\pi\pi}}. \quad (5.1)$$

From the right plots in Fig. 8, one can read off the values of η_R from the height of the curves at the resonances. The values agree with those shown in Table IV. Recall that for $\Gamma_R/m_R \ll 1$, we can approximate η_R by the integration of the normalized differential rate around the resonance as shown in Eq. (2.24). For example, for the $B^- \rightarrow R^0 \pi^- \rightarrow K^- \pi^+ \pi^-$ decays, η_R can be approximately given by

$$\eta_R \simeq \frac{\pi}{2 \tan^{-1} 2} \int_{m_R - \Gamma_R}^{m_R + \Gamma_R} \frac{d\tilde{\Gamma}(m_{K\pi})}{dm_{K\pi}} dm_{K\pi} = \frac{\pi}{2 \tan^{-1} 2} \left(1 - \int_{\text{elsewhere}} \frac{d\tilde{\Gamma}(m_{K\pi})}{dm_{K\pi}} dm_{K\pi} \right). \quad (5.2)$$

Note that for the case of η_ρ^{GS} one needs to include the $1/(1 + D \Gamma_\rho^0/m_\rho)^2$ factor. Numerically, we find that this approximation works well for the decay modes considered in this section. The above equation clearly shows that η_R represents the fraction of rates around the resonance and it is anticorrelated with the fraction of rates off the resonance.

From the Figs. 8(a) and (g), we see that for $R = \bar{K}^{*0}$ and ρ^0 the normalized differential rates predicted by QCDF are very similar to those obtained by using the experimental parameterization, while for $R = \bar{K}_0^{*0}$ and \bar{K}_2^{*0} the QCDF results and experimental models are different. Consequently, as shown in Figs. 8(b) and (h), QCDF and the experimental model give similar values on $d\tilde{\Gamma}(m_{\bar{K}^*})/dm_{K\pi}$ and $d\tilde{\Gamma}(m_\rho)/dm_{\pi\pi}$, resulting in $\eta_R^{\text{QCDF}} \simeq \eta_R^{\text{EXPP}}$ for $R = \rho$ and K^* . In contrast, as shown in Figs. 8(d) and (f), the QCDF $d\tilde{\Gamma}(m_{\bar{K}_0^*})/dm_{K\pi}$ and $d\tilde{\Gamma}(m_{\bar{K}_2^*})/dm_{K\pi}$ are smaller than those from the experimental model, resulting in $\eta_{K_0^*, K_2^*}^{\text{QCDF}} < \eta_{K_0^*, K_2^*}^{\text{EXPP}}$.

Using Eq. (5.2), we can relate the smallness of $\eta_{K_0^*}^{\text{QCDF}}$, comparing to $\eta_{K_0^*}^{\text{EXPP}}$, to the fact that the normalized differential rate obtained in the QCDF calculation is much larger than the one using the experimental parameterization in the off-resonance region, particularly in the large $m_{K\pi}$ region. To verify the source of the enhancement, we note that, as shown in Eq. (4.112), the $m_{K\pi}$ dependence in the QCDF amplitude is governed by the strong decay form factor, $F(m_{K\pi}^2, m_{K_0^*})$, the $B \rightarrow \pi$ form factor, $F_0^{B\pi}(m_{K\pi}^2)$, and a $m_{K\pi}^2$ factors sitting in front of the QCD penguin Wilson coefficient ($a_6^p - a_8^p/2$) and related to the so-called chiral factor (r_χ^S) in the two-body decay (see Eq. (4.113)). The last two factors are responsible for the enhancement of the QCDF differential rate in the large $m_{K\pi}$ region. As shown in Eq. (3.1) and the equations below it, these two factors are not included in the experimental parameterization for the scalar resonance. As a result, QCDF and the experimental parameterization give different normalized differential rates and η_R for this mode.

The momentum dependence (such as $m_{K\pi}$) of weak dynamics is mode-dependent. For example, in the above $B^- \rightarrow \overline{K}_0^*(1430)\pi^- \rightarrow K^-\pi^+\pi^-$ decay, we have a $m_{K\pi}^2$ factor from the chiral factor r_χ^S , while the chiral factor r_χ^V in the $B^- \rightarrow \overline{K}^*(980)\pi^- \rightarrow K^-\pi^+\pi^-$ decay does not provide the $m_{K\pi}^2$ factor (see Eq. (4.56)). Such a difference in the momentum dependence of weak dynamics has a visible effect on the shape of the normalized differential rates, as depicted in Figs. 8(a) and (c).

As shown in Eq. (3.1), the weak dynamics in the experimental parameterization is basically represented by a complex number, the coefficient c , which does not have any momentum dependence. In the narrow width limit, the value of the normalized differential rate is highly dominated by its peak at the resonance, and the values of the normalized differential rate elsewhere cannot compete with it. Therefore, only $m_{K\pi(\pi\pi)} \simeq m_R$ matters and, consequently, it is legitimate to use a momentum-independent coefficient, namely c , to represent the weak dynamics. However, in the case of a broad resonance, things are generally different. The peak at the resonance is no longer highly dominating, as its height is affected by the values of the normalized differential rate elsewhere. In this case, the momentum dependence of the weak dynamics cannot be ignored and, hence, using a momentum-independent coefficient to represent the weak dynamics is too naïve.

B. Branching fractions of quasi-two-body decays

For given experimental measurements of $\mathcal{B}(B^+ \rightarrow RP_3 \rightarrow P_1P_2P_3)$, we show in Table V various branching fractions of the quasi-two-body decays $B^+ \rightarrow RP_3$. $\mathcal{B}(B^+ \rightarrow RP_3)_{\text{NWA}}$ denotes the branching fraction obtained from Eq. (1.2) in the NWA. Our results of $\mathcal{B}(B^+ \rightarrow RP_3)_{\text{NWA}}$ for $B^+ \rightarrow K_2^{*0}(1430)\pi^+$, $K^{*0}\pi^+$, and $K^+\rho^0$ modes agree with the PDG data [3]. For $B^+ \rightarrow f_2(1270)\pi^+$, $\rho^0\pi^+$, and $\sigma\pi^+$ decays, we have included the new measurement of $B^+ \rightarrow \pi^+\pi^+\pi^-$ performed by the LHCb Collaboration [9, 10]. As for $\mathcal{B}(B^+ \rightarrow K_0^{*0}\pi^+)_{\text{NWA}}$, our value is different from $(39_{-5}^{+6}) \times 10^{-6}$ given by PDG [3] as the contribution of $B^+ \rightarrow K_0^{*0}\pi^+ \rightarrow K_S^0\pi^0\pi^+$ [38] is included in the latter case.

When the resonance is sufficiently broad, it is necessary to take into account the finite-width effects characterized by the parameter η_R . In Table V, we have shown the corrections to $\mathcal{B}(B^+ \rightarrow RP_3)_{\text{NWA}}$ in both QCDF and EXPP schemes. Although the finite-width effects are generally small, they are significant in the $B^+ \rightarrow \rho\pi^+$ decay and prominent in $B^+ \rightarrow \sigma/f_0(500)\pi^+$ and

TABLE V: Branching fractions of quasi-two-body decays $B^+ \rightarrow RP_3$ (in units of 10^{-6}) derived from the measured $B^+ \rightarrow RP_3 \rightarrow P_1P_2P_3$ rates. $\mathcal{B}(B^+ \rightarrow RP_3)_{\text{NWA}}$ denotes the branching fraction obtained from Eq. (1.2) in the narrow width approximation.

Mode	$\mathcal{B}(B^+ \rightarrow RP_3 \rightarrow P_1P_2P_3)_{\text{expt}}$	$\mathcal{B}(B^+ \rightarrow RP_3)_{\text{NWA}}$	$\eta_R^{\text{QCDF}} \mathcal{B}(B^+ \rightarrow RP_3)_{\text{NWA}}$	$\eta_R^{\text{EXPP}} \mathcal{B}(B^+ \rightarrow RP_3)_{\text{NWA}}$
$B^+ \rightarrow f_2\pi^+ \rightarrow \pi^+\pi^-\pi^+$	1.17 ± 0.20 [8–10]	2.08 ± 0.36	2.09 ± 0.36	1.95 ± 0.33
$B^+ \rightarrow K_2^{*0}\pi^+ \rightarrow K^+\pi^-\pi^+$	$1.85^{+0.73}_{-0.50}$ [12, 30]	$5.56^{+2.19}_{-1.50}$	$5.40^{+2.13}_{-1.46}$	$5.85^{+2.31}_{-1.58}$
$B^+ \rightarrow \rho^0\pi^+ \rightarrow \pi^+\pi^-\pi^+$	8.36 ± 0.77 [8–10]	8.36 ± 0.77	7.78 ± 0.72 (GS)	7.95 ± 0.73 (GS)
			9.28 ± 0.86 (BW)	
$B^+ \rightarrow K^+\rho^0 \rightarrow K^+\pi^+\pi^-$	3.7 ± 0.5 [12, 30]	3.7 ± 0.5	3.5 ± 0.5 (GS)	3.4 ± 0.5 (GS)
			4.2 ± 0.6 (BW)	
$B^+ \rightarrow K^{*0}\pi^+ \rightarrow K^+\pi^-\pi^+$	6.71 ± 0.57 [12, 30]	10.1 ± 0.8	10.7 ± 0.9	10.9 ± 0.9
$B^+ \rightarrow \sigma\pi^+ \rightarrow \pi^+\pi^-\pi^+$	3.83 ± 0.84 [9, 10]	5.75 ± 1.26	12.36 ± 2.71	9.44 ± 2.08
$B^+ \rightarrow K_0^{*0}\pi^+ \rightarrow K^+\pi^-\pi^+$	$27.9^{+5.6}_{-4.3}$ [12, 30]	45^{+9}_{-7}	37^{+8}_{-6}	50^{+10}_{-8}

$B^+ \rightarrow K_0^{*0}(1430)\pi^+$. For example, the PDG value of $\mathcal{B}(B^+ \rightarrow \rho\pi^+) = (8.3 \pm 1.2) \times 10^{-6}$ [3] should be corrected to $(7.7 \pm 1.1) \times 10^{-6}$ in QCDF or $(7.9 \pm 1.1) \times 10^{-6}$ in EXPP. The large width effects in the $\sigma/f_0(500)$ production imply that $B^- \rightarrow \sigma\pi^-$ has a large branching fraction of order 10^{-5} . More precisely, the LHCb value of $\mathcal{B}(B^+ \rightarrow \sigma\pi^+) = (5.8 \pm 1.3) \times 10^{-6}$ should be corrected to $(12.4 \pm 2.7) \times 10^{-6}$ in QCDF or $(9.4 \pm 2.1) \times 10^{-6}$ in EXPP.

VI. CONCLUSIONS

For the branching fractions of the quasi-two-body decays $\mathcal{B}(B \rightarrow RP_3)$ with R being an intermediate resonant state, it is a common practice to apply the factorization relation, also known as the narrow width approximation (NWA), to extract them from the measured process $B \rightarrow RP_3 \rightarrow P_1P_2P_3$. However, such a treatment is valid only in the narrow width limit of the intermediate resonance, namely $\Gamma_R \rightarrow 0$. In this work, we have studied the corrections to $\mathcal{B}(B \rightarrow RP_3)$ arising from the finite-width effects. We consider the parameter η_R which is the ratio of the three-body decay rate without and with the finite-width effects of the resonance. Our main results are:

- We have presented a general framework for the parameter η_R and shown that it can be expressed in terms of the normalized differential rate and is determined by its value evaluated at the resonance. Since the value of the normalized differential rate at the resonance is anticorrelated with the normalized differential rate off the resonance, it is the shape of the normalized differential rate that matters in the determination of η_R .
- In the experimental analysis of $B \rightarrow RP_3 \rightarrow P_1P_2P_3$ decays, it is customary to parameterize the amplitude as $A(m_{12}, m_{23}) = cF(m_{12}, m_{23})$, where the strong dynamics is described by the function F parameterized in terms of the resonance line shape, the angular dependence and Blatt-Weisskopf barrier factors, while the information of weak interactions is encoded in the complex coefficients c . We evaluate η_R in this experimentally motivated parameterization and in the theoretical framework of QCDF.

- In QCDF calculations, we have verified the NWA relation both analytically and numerically for some charged B decays involving tensor, vector and scalar resonances. We have introduced a form factor $F(s_{12}, m_R)$ for the strong coupling of $R(m_{12}) \rightarrow P_1 P_2$ when m_{12} is away from m_R . We find that off-shell effects are small in vector meson productions, but prominent in the $K_2^*(1430)$, $\sigma/f_0(500)$ and $K_0^*(1430)$ resonances.
- In principle, the two-body rates reported by experiments should be corrected using $\eta_R = \eta_R^{\text{EXPP}}$ in Eq. (1.4), as the data are extracted using the experimental parameterization. On the other hand, the experimental parameterization of the normalized differential rates should be compared with the theoretical predictions using QCDF calculations as the latter take into account the energy dependence of weak interaction amplitudes. In some cases, where η_R^{EXPP} are very different from η_R^{QCDF} , we note that using an energy-independent coefficient c , in the experimental parameterization, to represent the weak dynamics is too naïve. Moreover, systematic uncertainties in these experimental results after being corrected by η_R^{EXPP} are still underestimated.
- We have compared between η_R^{QCDF} and η_R^{EXPP} for their width dependence in Figs. 1–7. Numerical results are summarized in Table IV. In general, the two quantities are similar for vector mesons but different for tensor and scalar mesons. A study of the differential rates in Fig. 8 enables us to understand the origin of their differences. For example, the similar normalized differential rates for ρ and K^* at and near the resonance account for $\eta_{\rho, K^*}^{\text{QCDF}} \simeq \eta_{\rho, K^*}^{\text{EXPP}}$. In contrast, the $m_{K\pi}^2$ dependence associated with the penguin Wilson coefficients ($a_6^p - a_8^p/2$) in $B^- \rightarrow \bar{K}_0^*(1430)\pi^- \rightarrow K^- \pi^+ \pi^+$ yields a large enhancement in the QCDF differential rate in the large $m_{K\pi}$ distribution, rendering $\eta_{K_0^*}^{\text{QCDF}} < \eta_{K_0^*}^{\text{EXPP}}$.
- Finite-width corrections to $\mathcal{B}(B^+ \rightarrow RP)_{\text{NWA}}$, the branching fractions of quasi-two-body decays obtained in the NWA, are summarized in Table V for both QCDF and EXPP schemes. In general, finite-width effects are small, less than 10%, but they are prominent in $B^+ \rightarrow \sigma/f_0(500)\pi^+$ and $B^+ \rightarrow K_0^{*0}(1430)\pi^+$ decays.
- It is customary to use the Gounaris-Sakurai model to describe the line shape of the broad $\rho(770)$ resonance to ensure the unitarity far from the pole mass. If the relativistic Breit-Wigner model is employed instead, we find $\eta_\rho^{\text{BW}} > 1 > \eta_\rho^{\text{GS}}$ in both QCDF and EXPP schemes owing to the $(1 + D \Gamma_\rho^0/m_\rho)$ term in the GS model. For example, in the presence of finite-width corrections, the PDG value of $\mathcal{B}(B^+ \rightarrow \rho\pi^+) = (8.3 \pm 1.2) \times 10^{-6}$ should be corrected to $(7.7 \pm 1.1) \times 10^{-6}$ in QCDF and $(7.9 \pm 1.1) \times 10^{-6}$ in EXPP.
- The $\sigma/f_0(500)$ scalar resonance is very broad, and its line shape cannot be described by the familiar Breit-Wigner model. We have followed the LHCb Collaboration to use a simple pole model description. We have found very large width effects: $\eta_\sigma^{\text{QCDF}} \sim 2.15$ and $\eta_\sigma^{\text{EXPP}} \sim 1.64$. Consequently, $B^- \rightarrow \sigma\pi^-$ has a large branching fraction of order 10^{-5} .
- We have employed the Breit-Wigner line shape to describe the production of $K_0^*(1430)$ in three-body B decays and found large off-shell effects. The smallness of $\eta_{K_0^*}^{\text{QCDF}}$ relative to

$\eta_{K_0^*}^{\text{EXPP}}$ is ascribed to the fact that the normalized differential rate obtained in the QCDF calculation is much larger than that using the EXPP scheme in the off-resonance region. The large discrepancy between QCDF estimate and experimental data of $\Gamma(B^- \rightarrow \overline{K}_0^{*0} \pi^- \rightarrow K^- \pi^+ \pi^-)$ still remains an enigma.

- In the approach of QCDF, the calculated CP asymmetries of $B^- \rightarrow f_2(1270)\pi^-$, $B^- \rightarrow \sigma/f_0(500)\pi^-$ and $B^- \rightarrow K^- \rho^0$ agree with the experimental observations. The non-observation of CP asymmetry in $B^- \rightarrow \rho(770)\pi^-$ can also be accommodated in QCDF.

Acknowledgments

This research was supported in part by the Ministry of Science and Technology of R.O.C. under Grant Nos. MOST-106-2112-M-033-004-MY3 and MOST-108-2112-M-002-005-MY3.

-
- [1] H. Y. Cheng, “Comments on the quark content of the scalar meson $f_0(1370)$,” *Phys. Rev. D* **67**, 054021 (2003) [arXiv:hep-ph/0212361 [hep-ph]].
- [2] T. Huber, J. Virto and K. K. Vos, “Three-Body Non-Leptonic Heavy-to-heavy B Decays at NNLO in QCD,” [arXiv:2007.08881 [hep-ph]].
- [3] P. A. Zyla *et al.* [Particle Data Group], *Prog. Theor. Exp. Phys.* 2020, 083C01 (2020).
- [4] H. Y. Cheng, “Hadronic charmed meson decays involving axial vector mesons,” *Phys. Rev. D* **67**, 094007 (2003) [arXiv:hep-ph/0301198 [hep-ph]].
- [5] H. Y. Cheng, C. W. Chiang and C. K. Chua, “Width effects in resonant three-body decays: B decay as an example,” *Phys. Lett. B* **813**, 136058 (2021) [arXiv:2011.03201 [hep-ph]].
- [6] D. Asner, “Charm Dalitz plot analysis formalism and results: Expanded RPP-2004 version,” [arXiv:hep-ex/0410014 [hep-ex]].
- [7] G. J. Gounaris and J. J. Sakurai, “Finite-width corrections to the vector meson dominance prediction for $\rho \rightarrow e^+e^-$,” *Phys. Rev. Lett.* **21**, 244 (1968)
- [8] B. Aubert *et al.* [BaBar Collaboration], “Dalitz Plot Analysis of $B^+ \rightarrow \pi^+\pi^+\pi^-$ Decays,” *Phys. Rev. D* **79**, 072006 (2009) [arXiv:0902.2051 [hep-ex]].
- [9] R. Aaij *et al.* [LHCb Collaboration], “Observation of Several Sources of CP Violation in $B^+ \rightarrow \pi^+\pi^+\pi^-$ Decays,” *Phys. Rev. Lett.* **124**, 031801 (2020) [arXiv:1909.05211 [hep-ex]].
- [10] R. Aaij *et al.* [LHCb Collaboration], “Amplitude analysis of the $B^+ \rightarrow \pi^+\pi^+\pi^-$ decay,” *Phys. Rev. D* **101**, 012006 (2020) [arXiv:1909.05212 [hep-ex]].
- [11] J. R. Pelaez, “From controversy to precision on the sigma meson: a review on the status of the non-ordinary $f_0(500)$ resonance,” *Phys. Rept.* **658**, 1 (2016) [arXiv:1510.00653 [hep-ph]].

- [12] B. Aubert *et al.* [BaBar Collaboration], “Evidence for Direct CP Violation from Dalitz-plot analysis of $B^\pm \rightarrow K^\pm \pi^\mp \pi^\pm$,” Phys. Rev. D **78**, 012004 (2008) [arXiv:0803.4451 [hep-ex]].
- [13] M. Beneke, G. Buchalla, M. Neubert, and C.T. Sachrajda, “QCD factorization for $B \rightarrow PP$ decays: Strong phases and CP violation in the heavy quark limit,” Phys. Rev. Lett. **83**, 1914-1917 (1999) [arXiv:hep-ph/9905312 [hep-ph]]; “QCD factorization for exclusive, nonleptonic B meson decays: General arguments and the case of heavy light final states,” Nucl. Phys. B **591**, 313 (2000) [arXiv:hep-ph/0006124 [hep-ph]].
- [14] M. Beneke and M. Neubert, “QCD factorization for $B \rightarrow PP$ and $B \rightarrow PV$ decays,” Nucl. Phys. B **675**, 333 (2003) [arXiv:hep-ph/0308039 [hep-ph]].
- [15] H. Y. Cheng and K. C. Yang, “Charmless Hadronic B Decays into a Tensor Meson,” Phys. Rev. D **83**, 034001 (2011) [arXiv:1010.3309 [hep-ph]].
- [16] J. Tandean and S. Gardner, “Nonresonant contributions in $B \rightarrow \rho\pi$ decay,” Phys. Rev. D **66**, 034019 (2002) [arXiv:hep-ph/0204147 [hep-ph]]; S. Gardner and U. G. Meissner, “Rescattering and chiral dynamics in $B \rightarrow \rho\pi$ decay,” Phys. Rev. D **65**, 094004 (2002) [arXiv:hep-ph/0112281 [hep-ph]].
- [17] H. Y. Cheng and C. K. Chua, “Branching fractions and CP violation in $B^- \rightarrow K^+ K^- \pi^-$ and $B^- \rightarrow \pi^+ \pi^- \pi^-$ decays,” Phys. Rev. D **102**, 053006 (2020) [arXiv:2007.02558 [hep-ph]].
- [18] H. Y. Cheng, C. K. Chua and A. Soni, “Charmless three-body decays of B mesons,” Phys. Rev. D **76**, 094006 (2007) [arXiv:0704.1049 [hep-ph]].
- [19] H. Y. Cheng and C. K. Chua, “Branching Fractions and Direct CP Violation in Charmless Three-body Decays of B Mesons,” Phys. Rev. D **88**, 114014 (2013) [arXiv:1308.5139 [hep-ph]].
- [20] H. Y. Cheng, C. K. Chua and Z. Q. Zhang, “Direct CP Violation in Charmless Three-body Decays of B Mesons,” Phys. Rev. D **94**, 094015 (2016) [arXiv:1607.08313 [hep-ph]].
- [21] W. Wang, “B to tensor meson form factors in the perturbative QCD approach,” Phys. Rev. D **83**, 014008 (2011) [arXiv:1008.5326 [hep-ph]].
- [22] H. Y. Cheng, C. K. Chua, and C. W. Hwang, “Covariant light front approach for s wave and p wave mesons: Its application to decay constants and form-factors,” Phys. Rev. D **69**, 074025 (2004) [arXiv:hep-ph/0310359 [hep-ph]].
- [23] J. P. Dedonder, A. Furman, R. Kaminski, L. Lesniak and B. Loiseau, “ S -, P - and D -wave final state interactions and CP violation in $B^\pm \rightarrow \pi^\pm \pi^\mp \pi^\pm$ decays,” Acta Phys. Polon. B **42**, 2013 (2011) [arXiv:1011.0960 [hep-ph]].
- [24] H. Y. Cheng, C. K. Chua and A. Soni, “Final state interactions in hadronic B decays,” Phys. Rev. D **71**, 014030 (2005) [arXiv:hep-ph/0409317 [hep-ph]].
- [25] J. H. Alvarenga Nogueira, I. Bediaga, A. B. R. Cavalcante, T. Frederico and O. Lourenço, “CP violation: Dalitz interference, CPT, and final state interactions,” Phys. Rev. D **92**, 054010 (2015) [arXiv:1506.08332 [hep-ph]].
- [26] H. Y. Cheng, Y. Koike and K. C. Yang, “Two-parton Light-cone Distribution Amplitudes of Tensor Mesons,” Phys. Rev. D **82**, 054019 (2010) [arXiv:1007.3541 [hep-ph]].
- [27] M. Wirbel, B. Stech, and M. Bauer, “Exclusive Semileptonic Decays of Heavy Mesons,” Z. Phys. C **29**, 637 (1985); M. Bauer, B. Stech, and M. Wirbel, “Exclusive Nonleptonic Decays of D , D_s , and B Mesons,” Z. Phys. C **34**, 103 (1987).

- [28] H. Y. Cheng, “CP Violation in $B^\pm \rightarrow \rho^0\pi^\pm$ and $B^\pm \rightarrow \sigma\pi^\pm$ Decays,” [arXiv:2005.06080 [hep-ph]].
- [29] H. Y. Cheng and C. K. Chua, “Revisiting Charmless Hadronic $B_{u,d}$ Decays in QCD Factorization,” Phys. Rev. D **80**, 114008 (2009) [arXiv:0909.5229 [hep-ph]].
- [30] A. Garmash *et al.* [Belle Collaboration], “Evidence for large direct CP violation in $B^\pm \rightarrow \rho(770)^0 K^\pm$ from analysis of the three-body charmless $B^\pm \rightarrow K^\pm\pi^\pm\pi^\mp$ decay,” Phys. Rev. Lett. **96**, 251803 (2006) [hep-ex/0512066].
- [31] J. J. Qi, Z. Y. Wang, X. H. Guo and Z. H. Zhang, “Study of localized CP violation in $B^- \rightarrow \pi^-\pi^+\pi^-$ and the branching ratio of $B^- \rightarrow \sigma(600)\pi^-$ in the QCD factorization approach,” Nucl. Phys. B **948**, 114788 (2019) [arXiv:1811.10333 [hep-ph]].
- [32] H. Y. Cheng, C. K. Chua and K. C. Yang, “Charmless hadronic B decays involving scalar mesons: Implications to the nature of light scalar mesons,” Phys. Rev. D **73**, 014017 (2006) [arXiv:hep-ph/0508104].
- [33] R. Aaij *et al.* [LHCb Collaboration], “Dalitz plot analysis of $B^0 \rightarrow \overline{D}^0\pi^+\pi^-$ decays,” Phys. Rev. D **92**, 032002 (2015) [arXiv:1505.01710 [hep-ex]].
- [34] D. V. Bugg, “The Mass of the sigma pole,” J. Phys. G **34**, 151 (2007) [arXiv:hep-ph/0608081 [hep-ph]].
- [35] H. Y. Cheng, C. K. Chua, K. C. Yang and Z. Q. Zhang, “Revisiting charmless hadronic B decays to scalar mesons,” Phys. Rev. D **87**, 114001 (2013) [arXiv:1303.4403 [hep-ph]].
- [36] B. El-Bennich, A. Furman, R. Kaminski, L. Lesniak, B. Loiseau and B. Moussallam, “CP violation and kaon-pion interactions in $B \rightarrow K\pi^+\pi^-$ decays,” Phys. Rev. D **79**, 094005 (2009) [erratum: Phys. Rev. D **83**, 039903 (2011)] [arXiv:0902.3645 [hep-ph]].
- [37] D. Aston, N. Awaji, T. Bienz, F. Bird, J. D’Amore, W. Dunwoodie, R. Endorf, K. Fujii, H. Hayashi and S. Iwata, *et al.* “A Study of $K^-\pi^+$ Scattering in the Reaction $K^-p \rightarrow K^-\pi^+n$ at 11-GeV/c,” Nucl. Phys. B **296**, 493 (1988)
- [38] J. P. Lees *et al.* [BaBar Collaboration], “Evidence for CP violation in $B^+ \rightarrow K^*(892)^+\pi^0$ from a Dalitz plot analysis of $B^+ \rightarrow K_S^0\pi^+\pi^0$ decays,” Phys. Rev. D **96**, 072001 (2017) [arXiv:1501.00705 [hep-ex]].